# HIGH PRESSURE DIFFUSION COEFFICIENTS OF CARBON DIOXIDE IN THE IONIC LIQUID [bmim][$BF_4$]

by

Ömer Barış Emek

Submitted to the Institute of Graduate Studies in
Science and Engineering in partial fulfillment of
the requirements for the degree of Master of Science
in
Chemical Engineering

Yeditepe University

2014

HIGH PRESSURE DIFFUSION COEFFICIENTS OF CARBON DIOXIDE IN THE IONIC LIQUID [bmim][$BF_4$]

APPROVED BY:

Assist. Prof. Betül Üstünü .....

( Supervisor )

Prof. Salih Dinçer .....

Prof. Süheyla Uzman .....

DATE OF APPROVAL: 12/06/2014

# ACKNOWLEDGMENTS

I would like to express my gratitude to all those who gave me the possibility to complete this M.Sc. thesis. I am deeply indebted to my supervisor Assist. Prof. Betül Ünlüsü for her help, suggestions and encouragement during the research and writing of this thesis.

I would like to thank the Department of Chemical Engineering at Yeditepe University for their support and encouragement.

I am grateful to TUBİTAK for the financial supports provided (Project No. 110M457)

I would like to thank my labmates Melek Şekerci, and Emine Elif Avcı for the sleepless nights in laboratory.

I want to thank my family for their support, unlimited love, trust, and endless patience. They are the best parents that a person can have.

I also want to thank all my friends especially Deniz Halıcıoğlu, Okan Dede, Hakan Kına, Burak Erdoğan, Gözde Altun, Emre Kınacı, Burcu Erdoğan, Çağla Dereli, Poyraz Yılmaz, Uğur Dağ, Burhan Karakaş, Neslihan Kızılaslan, for their help and good friendship and not leaving me alone for all those years.

I want to send special thanks to my landlady, A. Melike Orhon, for opening her house to me and treating me as a child of hers and to my flat mates Umut Çetin and Serap Aktürk.

# ABSTRACT

## HIGH PRESSURE DIFFUSION COEFFICIENTS OF CARBON DIOXIDE IN THE IONIC LIQUID [bmim][$BF_4$]

The objective of this work is to determine the diffusion coefficients of the carbon dioxide-expanded ionic liquid systems at high pressure. The addition of high pressure carbon dioxide to a system containing an ionic liquid initiates one-way mass transfer: Carbon dioxide dissolves into the ionic liquid whereas the ionic liquid does not diffuse into carbon dioxide in measurable quantities. An experimental setup consisting of a high pressure view-cell where pressure and temperature are continuously monitored, a high pressure syringe pump for carbon dioxide loading at constant pressure, and a cathetometer to measure the changes in the liquid level has been built to determine the time dependent solubility values of carbon dioxide in the ionic liquid. The system is modeled as a Stefan problem which includes mass transfer between liquid and gas phases separated with a moving interface. Volume-of-fluid method is used to model the change in the position of the interface during the mass transfer process. The change in the density of the liquid during the process is also taken into account in the transport model. The increases in the diffusivities with the dissolution of carbon dioxide in the ionic liquid [bmim][$BF_4$], are determined at different temperatures (313.15 K, 323.15 K) and pressures (50-100 bar).

# ÖZET

## KARBONDİOKSİTİN [bmim][$BF_4$] İYONİK SIVISI İÇERİSİNDEKİ YÜKSEK BASINÇ YAYINIM KATSAYILARI

Bu çalışmanın amacı, yüksek basınçta karbondioksit gazı ile genleştirilmiş iyonik sıvı sistemlerinin yayınım katsayılarını belirlenmesidir. Iyonik sıvı içeren sisteme yüksek basınçta karbondioksit eklenmesi tek yönlü bir kütle aktarımı başlatır. Karbondioksit iyonik sıvı içerisinde çözünürken, iyonik sıvı karbondioksitin içine ölçülebilir miktarlarda taşınmaz. Karbondioksitin iyonik sıvı içerisindeki zamana bağlı çözünürlüğünü belirlemek için, sıcaklık ve basıncın sürekli izlendiği, dikey pencereli bir yüksek basınç hücresini, sabit basınçta karbondioksit yüklemesi yapabilen bir yüksek basınç şırınga pompasını ve sıvı seviyesindeki değişimi ölçmek için kullanılan bir katetometreyi içeren bir deney düzeneği kurulmuştur. Sistem, hareketli bir ara-yüzey tarafından ayrılmış sıvı ve gaz fazları arasındaki difüzyon sürecini kapsayan bir Stefan problemi olarak modellenmiştir. Kütle aktarım sürecinde fazlar arasındaki ara-yüzeyin konumunda oluşan değişim için "Akışkan Hacmi" yöntemi kullanılmış ve yine süreç sırasında sıvının yoğunluğunda gerçekleşen değişim modele eklenmiştir. [bmim][$BF_4$] iyonik sıvısı içerisinde karbondioksitin çözünmesiyle birlikte difüzyon katsayılarında oluşan artış farklı sıcaklık (313,15 K ve 323,15 K) ve basınçlarda (50-100 bar) belirlenmiştir.

# TABLE OF CONTENTS

# LIST OF FIGURES

# LIST OF TABLES

# LIST OF SYMBOLS / ABBREVIATIONS

| | |
|---|---|
| g | Gravitational Acceleration |
| n | Number of Moles |
| t | Time |
| u | Velocity |
| y | Mass Fraction |
| x | Mole Fraction |
| $\nabla x_i$ | Composition Gradient |
| | |
| D | Diffusion Coefficient |
| J | Diffusion Flux |
| P | Pressure |
| S | Source Term |
| $V_m$ | Molar Volume |
| | |
| $\gamma$ | Volume Fraction |
| $\eta$ | Viscosity of Liquid Phase |
| $\mu_t$ | Eddy Viscosity |
| $\mu$ | Viscosity |
| $\rho$ | Density |
| | |
| CXL | Carbon dioxide-Expanded Liquid |
| CFD | Computational Fluid Dynamics |
| GXL | Gas-Expanded Liquid |
| IL | Ionic Liquids |
| RTIL | Room Temperature Ionic Liquids |
| VOF | Volume of Fluid |

# 1. INTRODUCTION

Ionic liquids are organic salts, which are liquids at ambient temperatures. Unlike traditional solvents, which can be described as molecular liquids, ionic liquids are composed of ions. Their unique properties such as non-volatility, non-flammability, and excellent chemical and thermal stability have made them environmentally attractive solvents alternative to conventional organic solvents. Ionic liquids have low melting points (<100 ºC) and remain as liquids within a broad temperature window (<300 ºC) [1].

One obvious advantage of ionic liquids over organic solvents used commonly in industry is that the physical and chemical properties of the ionic liquids, including their polarity, hydrophobicity, viscosity, and solvent miscibility, can be fine-tuned by altering the cation, anion, and attached substituents. This is important, because by manipulating the solvent properties, one is allowed to design an ionic liquid for specific reaction conditions, where increasing the substrate solubility, modifying the enzyme selectivity, or tailoring the reaction rate are possible [1].

Ionic liquid-carbon dioxide systems are a unique sub-set of gas or carbon dioxide-expanded liquids. Carbon dioxide has high solubility in ionic liquids and decreases the viscosity of ionic liquids and increases their diffusivities [2]. Although, carbon dioxide is very soluble in the ionic liquid, in contrast, the ionic liquid is immeasurably insoluble in the pure carbon dioxide phase and they do not become miscible even at elevated pressures. This is different from the behavior of carbon dioxide with most organic solvents that are miscible at moderate pressures [2, 3].

In this study, high pressure diffusion coefficients have been determined for ionic liquid-carbon dioxide systems and the change in the binary diffusivities with the liquid mole fraction of carbon dioxide has been examined at different pressures and temperatures.

To determine the time-dependent volumetric expansion of liquid and carbon dioxide solubility, an experimental setup consisting of a jacketed high pressure view-cell equipped with a pressure transducer and a thermocouple, a high pressure syringe pump for carbon

dioxide loading at constant pressure or flow rate and water circulators connected to these units has been built. The changes in the phase-interface position with time are measured by using a cathetometer. The mole fractions of carbon dioxide in the ionic liquid and the molar volume of the ionic liquid-carbon dioxide mixture are determined by measuring the change in the interface position and volume of the carbon dioxide sent from high pressure syringe pump into the view-cell.

This thesis includes theoretical background on ionic liquids, gas-expanded liquids and the principles of computational fluid dynamics. The experimental set-up and procedure and the transport model are presented in Section 3. Section 4 includes results and discussion. Finally, conclusions drawn from results are explained in Section 5.

# 2. THEORETICAL BACKGROUND

This section includes theoretical background about ionic liquids, supercritical fluids, gas-expanded liquids, computational fluid dynamics and previous studies about ionic liquid-carbon dioxide systems.

## 2.1. IONIC LIQIDS

Ionic liquids (ILs) are known as salts that are liquid at room temperature in contrast to high-temperature molten salts. They have a unique array of physicochemical properties which make them suitable in numerous applications in which conventional organic solvents are not sufficiently effective or not applicable [2]. ILs have been accepted as a new green chemical revolution which excited both the academia and the chemical industries. This new chemical group can reduce the use of hazardous and polluting organic solvents due to their unique characteristics as well as taking part in various new syntheses [4].

Although ILs are known for a long time, using them as solvents in chemical processes for synthesis and catalysis has become significant in recent years. Although, some ILs were known even back in 1910s, the first intentional synthesis was carried out in 1970s for nuclear warheads batteries [5, 6]. During 1940s, aluminum chloride-based molten salts were utilized for electroplating at temperatures of hundreds of degrees Celsius. In the early 1970s, Wilkes tried to develop better batteries for nuclear warheads and space probes which required molten salts to operate [6]. These molten salts were too hot so they damaged the nearby materials. Therefore, the researchers looked for salts which remained liquid at lower temperatures and eventually they identified one which was liquid at room temperature. Wilkes and his colleagues continued to improve their ILs for use as battery electrolytes and then, a small community of researchers began to make ILs and test their properties [2, 6]. In the late 1990s, ILs became one of the most promising chemicals as solvents. Studying with ILs is considered as a young field, so the researchers still evaluate the some basic physical properties of ILs, such as viscosity and density [2]. As a result, the number of research studies on ILs is increasing rapidly.

For the future of ILs, the objective is to commercialize ILs in order to use them as solvents, reagents, catalysts and materials in large scale chemical applications.

### 2.1.1. Properties of Ionic Liquids

ILs are made of positively and negatively charged ions, whereas organic solvents are made of molecules. Their structure is similar to the table salt. While salts do not melt below 800°C, most of ILs remain liquid at room temperature. Since these conventional molten salts exhibit high melting points, their use as solvents in applications is severely limited. However, RTILs are liquid generally up to 200°C [2]. Researchers explained that ILs remain liquid at room temperature due to the reason that their ions do not pack well [7]. The low melting points of ILs are a result of the chemical composition. The combination of larger asymmetric organic cation and smaller inorganic counterparts lower the lattice energy and hence the melting point of the resulting ionic medium [2].

ILs are introduced as green solvents because unlike the volatile organic compounds, many of these compounds have negligible vapor pressure, they are not explosive and it may be feasible to recycle and reuse them. ILs are more convenient to work in the laboratory since their non-evaporating properties eliminate the hazardous exposure and air pollution problems.

ILs are also known as ‘designer solvents’ since they give the opportunity to tune their specific properties for a particular need. The researchers can design a specific IL by choosing negatively charged small anions and positively charged large cations, and these specific ILs may be utilized to dissolve a certain chemical or to extract a certain material from a solution. The fine-tuning of the structure provides tailor-designed properties to satisfy the specific application requirements. The physical and chemical properties of ILs are varied by changing the alkyl chain length on the cation and the anion [2].

ILs have been considered to be scarce but it is now known that many salts form liquids at or close to room temperature. There are billions of different structures that may form an IL. The composition and the specific properties of these liquids depend on the type of cation

and anion in the IL structure. By combining various kinds of cation and anion structures, it is estimated that $10^{18}$ ILs can be designed [8].

1-butyl-3 methylimidazolium tetrafluoroborate [bmim][$BF_4$] is one of the most common and studied ionic liquid. As most of the ionic liquids, [bmim][$BF_4$] is highly viscous, has very low vapor pressure, poor conductor. [bmim][$BF_4$] is considered as an environmentally friendly solvent, since it is non-volatile, non-flammable and has high chemical and thermal stability. It is liquid in a wide range from -75 °C to 290 °C. [bmim][$BF_4$] is colorless, and non-water soluble. It slowly decomposes in water. The structure of [bmim][$BF_4$] can be seen in Figure 2. 1.

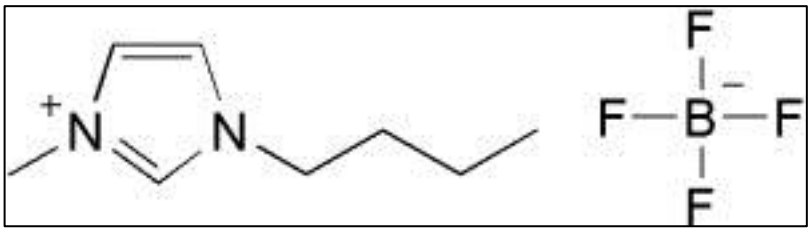


Figure 2.1. Molecular Structure of [bmim][$BF_4$]

Most commonly used ILs posses several advantages over conventional organic solvents, which make them environmentally compatible [1, 2, 4, 8];

- ILs have the ability to dissolve many different organic, inorganic and organometallic materials.
- ILs are highly polar.
- ILs consist of loosely coordinating bulky ions.
- ILs do not evaporate since they have very low vapor pressures.
- ILs are thermally stable, approximately up to 300 °C.
- Most of ILs have a liquid window of up to 200 °C which enables wide kinetic control.
- ILs have high thermal conductivity and a large electrochemical window.
- ILs are immiscible with many organic solvents.
- ILs are non-aqueous polar alternatives for phase transfer processes.

- The solvent properties of ILs can be tuned for a specific application by varying the anion cation combinations

### 2.1.2. Applications of Ionic Liquids

The application areas of ILs can be expressed as solvents for organic, organometallic synthesis and catalysis; electrolytes in electrochemistry, in fuel and solar cells; lubricants; stationary phases for chromatography; matrices for mass spectrometry; supports for the immobilization of enzymes; in separation technologies; as liquid crystals; templates for synthesis nano-materials and materials for tissue preservation; in preparation of polymer–gel catalytic membranes; in generation of high conductivity materials [10].

The major applications suggested for ILs;

- For purification of gases; studies show that some gases, especially $CO_2$ is highly soluble in ILs. The simulations performed explain that the anion of the IL is responsible for high gas solubility. With this property ILs, can be replaced as solvents in reactions involving gaseous species. Since ILs can dissolve certain gaseous species, they may be used in conventional gas absorption applications. The non-volatility of ILs prevents any cross contamination of the gas stream by the solvent during the process. Moreover, regeneration of the solvent may be performed easily by a simple flash or distillation to remove the gas from the solvent without any cross contamination [10].
- For solvent replacement; majority of common solvents have potential health hazards. Therefore, environmentally friendly ILs can replace hazardous solvents. ILs are able to dissolve various solutes so they can be used instead of traditional solvents [11].
- For homogenous and heterogeneous catalysts; ILs may be immiscible with the reactants and products but they may dissolve the catalysts. ILs combine the advantages of a solid for immobilizing the catalyst and a liquid for allowing the catalyst to move freely [12].

- For biological reaction media; ILs can be used as biological reaction media due to the stability of enzymes in ILs, and in separation processes such as extraction of amino acids [13].

## 2.2. SUPERCRITICAL FLUIDS

Supercritical fluid is a distinct state of matter that has properties of both a liquid and a gas. A supercritical gas may be regarded as an intermediary state between liquids and gases. Supercritical gases are only created above a material's thermodynamic critical point. This usually means high pressures, often between about 40 and 80 atmospheres, though it varies greatly. Some critical points, most notably water, are as high as 218 atmospheres and beyond. Supercritical fluids have low viscosities and high diffusivities. Supercritical gases can diffuse into and through solids like a gas, but also dissolves certain materials like a liquid. [14].

In 1822, Baron Charles Cagniard de la Tour discovered supercritical fluids while conducting experiments involving the discontinuities of the sound of a flint ball in a sealed cannon barrel filled with various fluids at various temperatures [15].

The phenomenon can be easily explained with reference to the phase diagram for pure carbon dioxide (see Figure 2.2).

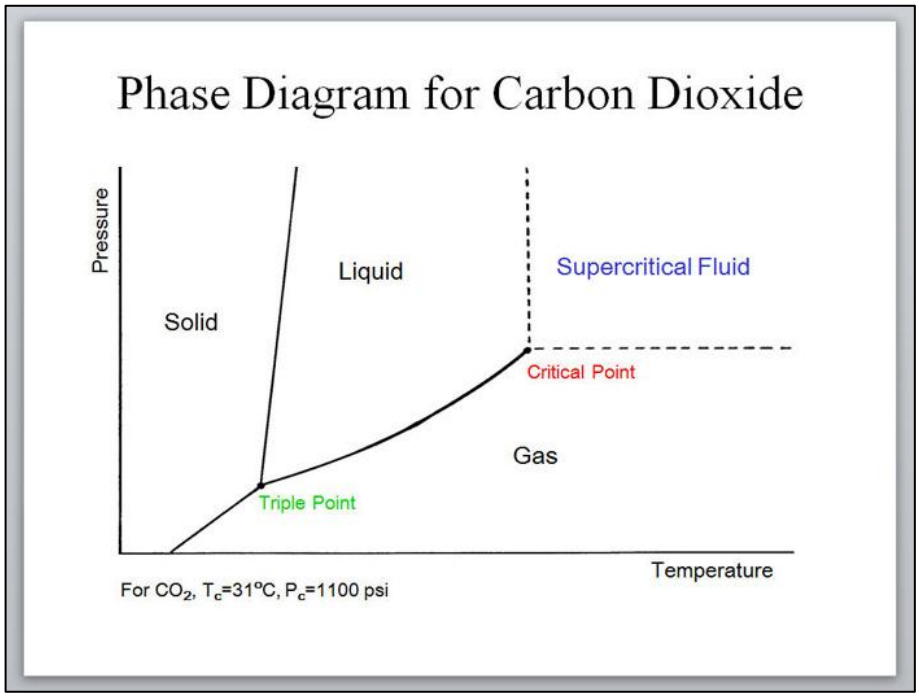


Figure 2.2 Phase Diagram of Pure Carbon dioxide [17]

This figure shows the areas where carbon dioxide exists as a gas, liquid, solid or as a supercritical fluid. The curves represent the temperatures and pressures where two phases coexist in equilibrium (at the triple point, the three phases coexist). The gas-liquid coexistence curve is known as the boiling curve. Moving upwards along the boiling curve, increasing both temperature and pressure, then the liquid becomes less dense due to thermal expansion and the gas becomes more dense as the pressure rises. Eventually, the densities of the two phases converge and become identical, the distinction between gas and liquid disappears, and the boiling curve comes to an end at the critical point. The critical point for carbon dioxide occurs at a pressure of 73.8 bar and a temperature of 31.1°C [16].

Any commercialization of a process that uses supercritical fluids must involve a cost analysis that should indicate the advantages in the new process offsets the penalty of high pressure operations. A variety of supercritical fluid processes have been commercialized. Many other processes have been investigated on a lab or pilot plant scale and have the potential to be scaled up in the near future [16].

## 2.3. GAS-EXPANDED LIQUIDS

Gas-expanded liquid (GXL) is a mixed solvent composed of a compressible gas dissolved in an organic solvent. $CO_2$–expanded liquids (CXLs) are most commonly used GXLs [14]. The presence of dissolved gas results in improved transport properties and increased solubility of permanent gases such as $O_2$, CO and $H_2$.

Compared to conventional solvent systems, adjusting the pressure of the compressed gas varies its introduction into liquid phase and thereby allows tunability of the properties of the GXL phase. For example, viscosities and interfacial tension decrease and diffusivity increases, while solubilities of permanent gases can increase compared to organic solvents [17].

Due to its economic advantages and low risk associated with its use, $CO_2$ is usually used as compressible gas. $CO_2$ enhances gas solubility and mass transfer, while organic solvents increase the solubility of liquid and solid solutes. The properties of gas-expanded solvent can be tuned by exploiting the properties of the organic solvent and those of the gas, simply varying the pressure of the system [18].

### 2.3.1. Carbon dioxide-Expanded Liquids

Carbon dioxide-expanded liquids (CXLs) are the most common class of GXLs. Its low cost and being safe provide this title.

If $CO_2$ is present during a reaction in a liquid solvent, then the presence of $CO_2$ can have substantial effect on the reaction rate. Dissolution of $CO_2$ into liquid phase above 40 bars causes an observable and typically multi-fold increase in the volume of the liquid phase, accompanied by changes in the physical properties of the liquid mixture [17].

Different liquids expand differently in the presence of $CO_2$ pressure. Liquids are divided into three classes by the ability to dissolve $CO_2$.

Class 1 liquids; this liquids barely dissolve $CO_2$ and do not expand significantly. Also they have no essential change in their properties except acidity. Water is an example for this class.

Class 2 liquids such as methanol, hexane and many other organic solvents, dissolve large amount of $CO_2$ and expand greatly. They have significant change in physical properties.

Class 3 liquids such as ionic liquid, liquid polymers and crude oil, dissolve only moderate amount of $CO_2$ and expand moderately in volume. Some properties such as viscosity and diffusivity change significantly while others, such as polarity do not change [18].

## 2.4. COMPUTATIONAL FLUID DYNAMICS

Computational fluid dynamics, usually abbreviated as CFD, is a branch of fluid mechanics that uses numerical methods and algorithms to solve and analyze problems that involve fluid flows. The basic principle of the CFD modeling method is simple. The flow regime is divided into small cells within each of which the flow either kept constant or varies smoothly. The differential equations of momentum, energy, and mass balance are discretized and represented in terms of the variables at the cell centers or at a predetermined position within the cells [19].

CFD modeling provides a good description of flow field variables, velocities, temperature, or a mass concentration anywhere in the region with details not usually available through physical modeling [20].

There are many advantages in considering computational fluid dynamics. Firstly, the theoretical development of the computational sciences focuses on the construction and solution of the governing equations and study of various approximations to these equations. CFD presents the perfect opportunity to study specific terms in the governing equations in a more detailed fashion. New paths of theoretical development are realized, which could not have been possible without the introduction of this branch of computational approach. Secondly, CFD complements experimental and analytical approaches by providing an alternative cost-effective means of simulating real fluid flows.

Thirdly, CFD has the capacity of simulating flow conditions that are not reproducible in experimental test found in geophysical and biological fluid dynamics, such as nuclear accident scenarios or scenarios that are too huge or too remote to be simulated experimentally (e.g., Indonesian Tsunami of 2004). Fourthly, CFD can provide rather detailed, visualized, and comprehensive information when compared to analytical and experimental fluid dynamics [21].

In computational fluid dynamics, the volume of fluid method (or in short VOF method) is a numerical technique for tracking and locating the free surface (or fluid-fluid interface). It belongs to the class of Eulerian methods which are characterized by a mesh that is either stationary or is moving in a certain prescribed manner to accommodate the evolving shape of the interface. As such, VOF is an advection scheme, a numerical recipe that allows the programmer to track the shape and position of the interface, but it is not a standalone flow solving algorithm [22].

The VOF technique can model two or more immiscible fluids by solving a single set of momentum equations and tracking the volume fraction of each of the fluids throughout the domain. Typical applications include the prediction of jet breakup, the motion of large bubbles in a liquid, the motion of the liquid after a dam break, and the steady or transient tracking of any liquid-gas interface [22].

The VOF method is a surface-tracking technique applied to a fixed Eulerian mesh, in which a specie transport equation is used to determine the relative volume fraction of the two phases, or phase fraction, in each computational cell. Practically, a single set of Reynolds averaged Navier-Stokes equations is solved and shared by the fluids and for the additional phase, its volume fraction γ is tracked throughout the domain [23].

Therefore, the full sets of governing equations for the fluid flow are;

$$\nabla.u=0 \tag{2.1}$$

$$\rho \frac{Du}{Dt} = -\nabla P + \rho g + \mu \nabla^2 u \tag{2.2}$$

$$\frac{\partial \gamma}{\partial t}+\nabla.(u\gamma)=0 \tag{2.3}$$

Where u is the velocity vector field, P is the pressure field $\mu_t$ is the turbulent eddy viscosity.

For the incompressible phase volume fraction, $\gamma$, the following three conditions are possible;

- $0<\gamma<1$: when the infinitesimal volume contains the interface between the q-th fluid and one or more other fluids;
- $\gamma=0$: volume occupied by air;
- $\gamma=1$: volume occupied by water.

The nature of the VOF method means that an interface between the species is not explicitly computed, but rather emerges as a property of phase fraction field. Since the phase fraction can have any value between 0 and 1, the interface is never sharply defined, but occupies a volume around the region where a sharp interface should exist [24].
Physical properties are calculated as weighted averages based on this fraction. The density and viscosity in the domain are, therefore, calculated as follows:

$$\rho=\gamma\rho_1+(1-\gamma)\rho_2 \tag{2.4}$$

$$\mu=\gamma\mu_1+(1-\gamma)\mu_2 \tag{2.5}$$

Where, subscript 1 and 2 refer to the gas and the liquid respectively.

The following restrictions apply to the VOF model in FLUENT:

- Pressure-based solver must be used. The VOF model is not available with density-based solver
- All control volumes must be filled with either a single fluid phase or a combination of phases. The VOF model does not allow for void regions where no fluid of any type is present.

- Only one of the phases can be defined as a compressible ideal gas. There is no limitation on using compressible liquids using user-defined functions.
- Stream wise periodic flow (either specified mass flow rate or specified pressure drop) cannot be modeled when the VOF model is sued
- The second order implicit time stepping formulation cannot be used with the VOF explicit scheme [22].

## 2.5. IONIC LIQUID-CARBON DIOXIDE SYSTEMS

Moganty and Baltus used a transient thin liquid film gas uptake technique to measure the diffusion coefficients of carbon dioxide under infinite dilution conditions in eight commercially available room-temperature ionic liquids at 10, 25, and 40 °C. The measured $CO_2$ diffusion coefficients were $1 \times 10^{-6}$ $cm^2/s$, an order of magnitude smaller than coefficients for $CO_2$ diffusion in traditional organic solvents. Combining these results with diffusivity values reported in the literature for $CO_2$ diffusivity in nonionic fluids shows a generally universal relationship between diffusivity and solvent viscosity, with diffusivity inversely proportional to the square root of viscosity. Results were used to develop correlations relating $CO_2$ diffusion to ionic liquid properties and system temperature [27].

Shokouhi et al. determined the solubilities and diffusion coefficients of hydrogen sulfide and carbon dioxide gases in the ionic liquid [hemim][$BF_4$], at temperatures ranging from (303.15 to 353.15 K) and pressures up to 1.1 mPa. The diffusion coefficients were obtained for $H_2S$ and $CO_2$ using a semi-infinite volume approach and a correlation equation with temperature is presented for each gas. [28].

Hou et al. reported the results from an experimental investigation of carbon dioxide solubility and diffusivity in the ionic liquids [bmim][$Tf_2N$], [pmmim][$Tf_2N$], [bmpy][$Tf_2N$], [perfluoro-hmim][$Tf_2N$], and [bmim][$BF_4$]. A transient thin liquid film method was developed, which enables one to determine the Henry's law constant and the diffusivity at low pressure simultaneously. Measurements were performed at temperatures in the range of 283−323 K. The measured $CO_2$ diffusion coefficients in the five ionic liquids were on the order of $10^{-6}$ $cm^2/s$, which is an order of magnitude smaller than the coefficients for $CO_2$ diffusion in traditional organic solvents. In contrast to the gas

solubility results, measured diffusion coefficients were determined to be dependent on the ionic liquid cation as well as the anion. In addition, $CO_2$ diffusion coefficients were considerably more sensitive to temperature than were $CO_2$ solubilities in these ionic liquids. Results were used to develop a correlation relating $CO_2$ diffusion to ionic liquid properties and system temperature [29].

Condemarin and Scovazzo reported diffusivities over a range of viscosities (71–532 cP) and develop a predictive diffusivity correlation. They reported the permeability, solubility, and diffusivity data for nine gases in nine ammonium based RTILs at 30°C, as determined with a lag-time technique. They generated a membrane system by fixing ionic liquid in a glass fiber porous base, so the mass fraction was reduced to only molecular diffusion. Lag-time technique measures the outlet pressure of the membrane with respect to time. These values are used in the equation derived from Fick's Law of Diffusion to determine the diffusion coefficient. In this study, diffusion coefficients of carbon dioxide in imidazolium, phosphonium and ammonium based ionic liquids were determined [30].

Shiflett and Yokozeki reported that carbon dioxide absorption measurements in ([bmim][$PF_6$]) and ([bmim]-[$BF_4$]) were made using a commercial gravimetric microbalance at temperatures of 283.15, 298.15, 323.15, and 348.15 K and at pressures under 2 MPa. Equation of state model was used to predict some phase behaviors of $CO_2$ and ionic liquid mixtures as well as Henry's law constants and the volume change of solutions. To obtain binary diffusion coefficients of $CO_2$ in the ionic liquids from time-dependent absorption data, simple diffusion model was used [31].

Xu et al. reported that Molecular dynamics simulation with an all-atom force field has been carried out on the two binary systems of [bmim][$PF_6$]-$CO_2$ and [bmim][$NO_3$]-$CO_2$ to study the transport properties, volume expansion and microstructures. It was found that addition of $CO_2$ in the liquid phase could greatly decrease the viscosity of ionic liquids and increase their diffusion coefficient obviously. Furthermore, the volume expansion of ionic liquids was found to increase with the increase of the mole fraction of $CO_2$ in the liquid phase but less than 35% for the two simulated systems, which had a significant difference with $CO_2$ expanded organic solvents [32].

# 3. EXPERIMENTAL SET- UP AND TRANSPORT MODEL

In this section, the experimental set-up, procedure of the experiments and the transport model are explained in detail.

## 3.1. THE EXPERIMENTAL SET-UP AND PROCEDURE

The experimental system is shown in Figure 3.1

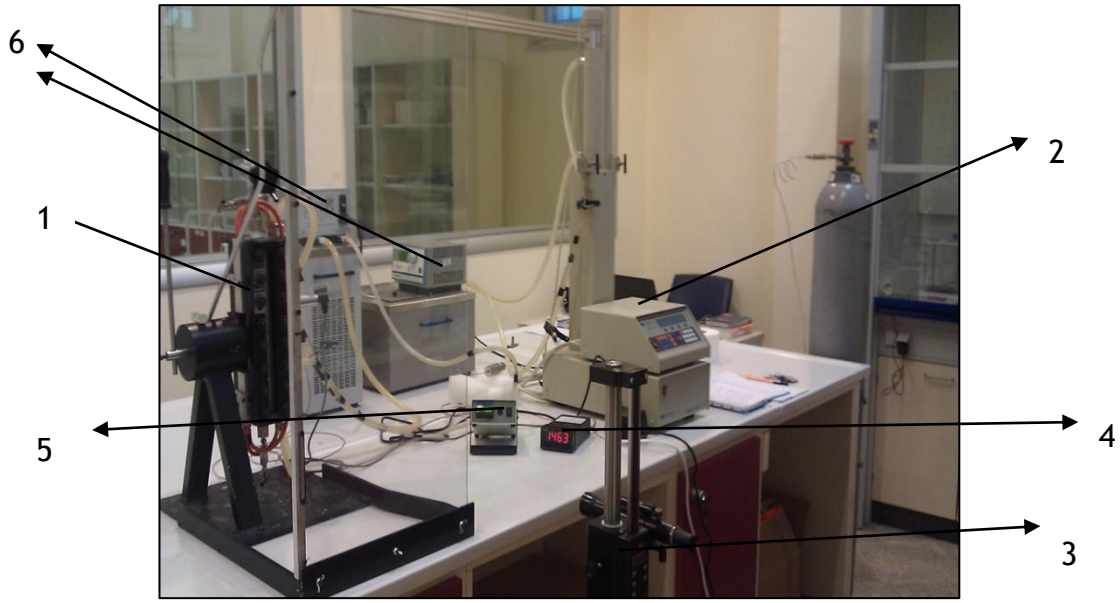


Figure 3.1 Experimental Set-Up

The system consists of the following instruments

1. Jerguson high pressure cell
2. ISCO high pressure syringe pump
3. Cathetometer
4. Pressure transducer
5. Thermocouple
6. Water circulators

Before each high pressure experiment, any possible carbon dioxide leakage in the system is checked. First, the view-cell is tested whether it can hold a pressure of 1500 psia (103.4 bar), by monitoring the transducer connected to the cell after carbon dioxide loading. If the pressure stays constant, then the line between the pump and the view-cell, and finally, the pump itself are tested.

The moisture content in the ionic liquid can affect the solubility of carbon dioxide. [bmim] [$BF_4$] is highly hygroscopic and therefore, the amount of water in the ionic liquid samples is measured before the experiments using Karl-Fischer instrument. The results are all below 400 ppm, which is a sufficiently low value.

After these pre-experimental tests, the syringe pump is filled with liquid carbon dioxide at 10 $^{o}$C. When it is full, the temperature and pressure of the pump are set to the desired values for that run. Then, the line between the pump and the view-cell is filled with $CO_2$ by opening the outlet valve of the pump. The next step is to place the ionic liquid sample into the view-cell via the bottom valve and to wait a certain amount of time for the temperature of the liquid to reach that of the system. Then, the cathetometer is adjusted to ionic liquid's meniscus. After recording all initial readings, the view-cell is loaded with carbon dioxide and the diffusion process gets started. As the dissolution takes place, the liquid level increases and carbon dioxide volume in the pump decreases. These data are recorded at a constant time interval until equilibrium. After recording final readings, the inlet valve of the cell is closed and outlet valve is opened slowly. It is important that releasing high pressure $CO_2$ with very slow flow rate to avoid any accidents. Once the cell pressure drops to the room pressure, it is safe to open the bottom valve and remove the ionic liquid from the cell. Finally, the high pressure cell is washed with ethanol and left for drying at 70 $^{o}$C.

### 3.2. THE TRANSPORT MODEL

Adding high pressure carbon dioxide to an ionic liquid system initiates one way mass transfer. Carbon dioxide dissolves in the ionic liquid while the ionic liquid does not diffuse into the vapor phase in measurable quantities. Therefore, our system consists of two phases separated with a moving boundary. As shown in figure 3.2, the phase-interface is moving upward as carbon dioxide diffuses into the liquid.

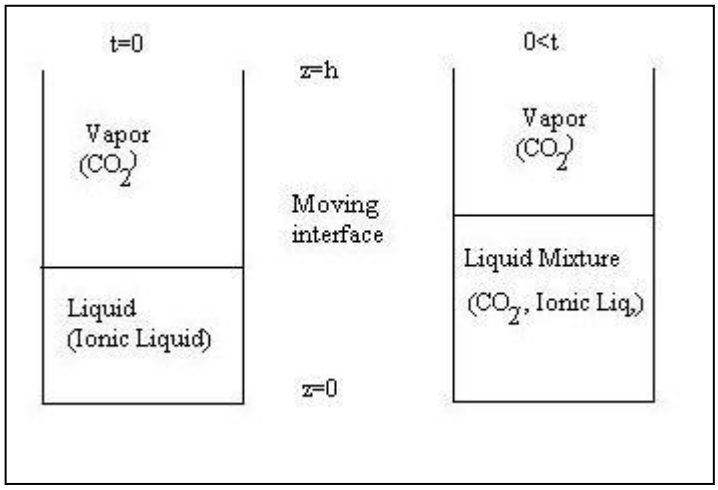


Figure 3.2. Model of Ionic Liquid- Carbon dioxide System

A commercial computational fluid dynamics (CFD) software, Fluent, is used for modeling of this process. The Volume of Fluid (VOF) technique is used in Fluent for expressing the moving interface mathematically. In this method, a function, that shows the volume fraction of one phase in every cell of the mesh, is defined ($\alpha_q$) [34, 35, 36].

Tracking of the phase interface can be done by solving the equation 3.2

$$\frac{1}{\rho_q}\left[\frac{\partial(\alpha_q\rho_q)}{\partial t}+\nabla.(\alpha_q\rho_q u)\right]=S_{\alpha q} \tag{3.2}$$

Where, ρ is the density and u is the velocity of q phase.

If there is no q phase in a cell, $\alpha_q$ is equal to 0. If there is only q phase, $\alpha_q$ is equal to 1. If $\alpha_q$ is between 0 and 1, that means the interface is passing through the cell. Because of the mass transfer between phases, the source term, $S_{\alpha q}$, takes a value other than 0. The source term is calculated by equation 3.3 based on mass transfer in liquid phase.

$$S_{\alpha L}=-\rho_L D\nabla y^{CO_2}.\nabla\alpha_L \tag{3.3}$$

Equal amount of mass loss will occur in the gas phase.

$$S_{\alpha G}=-S_{\alpha L} \tag{3.4}$$

In VOF method, equation 3.5, where P is pressure, g is gravitational acceleration and μ is viscosity, is used for the entire domain.

$$\frac{\partial(\rho u)}{\partial t}+\nabla.(\rho uu)=-\nabla P+\mu\nabla^2 u+\rho g \tag{3.5}$$

Transport of carbon dioxide is expressed using equation 3.6. In this equation $y_q^{CO_2}$ is the mass fraction of carbon dioxide in the $q^{th}$ phase, $J_q^{CO_2}$ is the diffusion flux of carbon dioxide in this phase and $S^{CO_2}$ is the source term for carbon dioxide.

$$\frac{\partial\left(\rho_q \alpha_q y_q^{CO_2}\right)}{\partial t}+\nabla.\left(\rho_q \alpha_q u y_q^{CO_2}\right)=-\nabla\left(\alpha_q J_q^{CO_2}\right)+S^{CO_2} \tag{3.6}$$

Diffusion flux is expressed as;

$$J^{CO_2}=-D\nabla(\rho y^{CO_2}) \tag{3.7}$$

As seen in equation 3.3, while calculating mass transfer between phases, mass fraction gradient is needed at the phase interface. However, in Fluent, transport equations for components are solved separately for each phase. Hence, a discontinuity in the liquid carbon dioxide mass fraction gradient occurs at the interface and mass transfer value becomes physically wrong here. A user defined scalar (φ) for the entire flow domain is defined to overcome this problem. The scalar shared by both phases and the following transport equation is solved for the whole domain.

$$\frac{\partial(\rho\varphi_k)}{\partial t}+\nabla.(\rho u\varphi_k)=-\nabla.(J_{\varphi_k})+S_{\varphi_k} \tag{3.8}$$

The value of the scalar is equal to the mass fraction at the interface (equilibrium mass fraction of carbon dioxide in ionic liquid at that pressure and temperature) in all of the cells partially or completely filled with the gas phase. These cells need to keep the same mass

fraction and to ensure this, a method, called internal boundary condition, is used, where the transport equation is made completely dominated by a source term, defined in equation 3.9, which is assigned an exceptionally large value in the gas phase. However, the source term is assigned zero in the liquid phase [34, 35].

$$S_{\varphi_k} = A(\varphi_{k,eq} - \varphi_k) \tag{3.9}$$

# 4. RESULTS AND DISCUSSION

In this section, the experimental mole fractions of carbon dioxide in the liquid phase and the corresponding modeling results, the increase in the liquid levels, liquid molar volumes and the calculated diffusivities are presented at different pressures (50-100 bar) and temperatures (313.15 K and 323.15 K) for [bmim][$BF_4$]-$CO_2$ system.

## 4.1. [bmim][$BF_4$] – $CO_2$ SYSTEM AT 313.15 K AND 739 PSIA (50.9 BAR)

The data for the experimental run is presented below. Liquid level and the mole fraction of $CO_2$ in liquid increase and reach equilibrium as expected (see figures 4.1 and 4.2). Mole fraction at equilibrium is found to be 0.392. This value is calculated using the increase in the liquid level, measured using the cathetometer, and the volume reading from the high pressure pump. A sample calculation for the equilibrium mole fraction is presented in Appendix A. The change in the liquid molar volume during the dissolution of carbon dioxide, and the diffusion coefficients obtained by fitting the model to the experimental data are shown in Figures 4.3 and 4.4 respectively.

- Mass of the ionic liquid in the system: 8.4874 g
- Volume of carbon dioxide loaded to the system: 146.85 ml
- Initial volume of carbon dioxide in syringe pump: 256.62 ml
- Final volume of carbon dioxide in syringe pump: 101.81 ml
- Pressure of the system during the experiment: 739 ± 2 psia
- Temperature of the system during the experiment: 40.0 ± 0.1 $^0$C

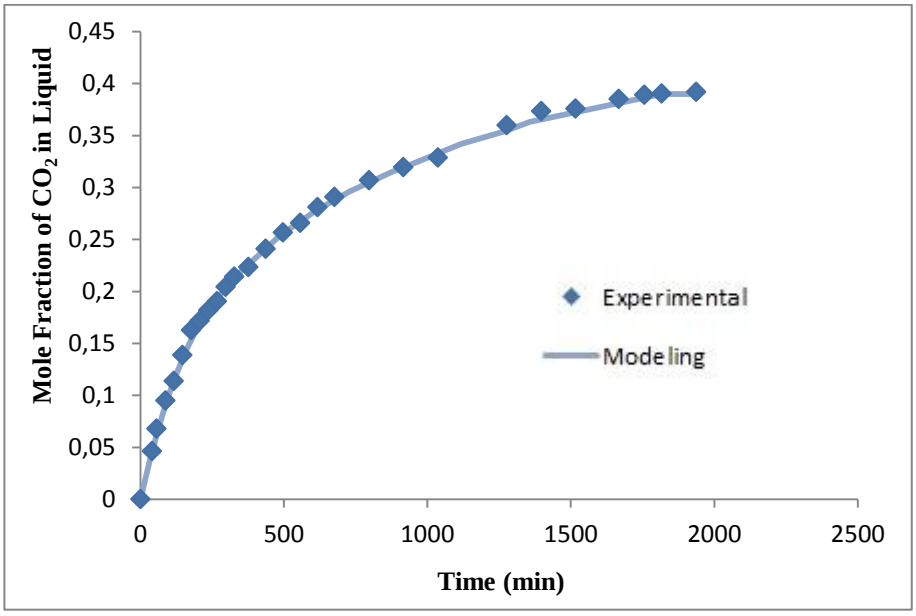


Figure 4.1. Average Carbon dioxide Mole Fractions in the Liquid Phase (40 $^{o}$C and 739 psia (50.9 bar))

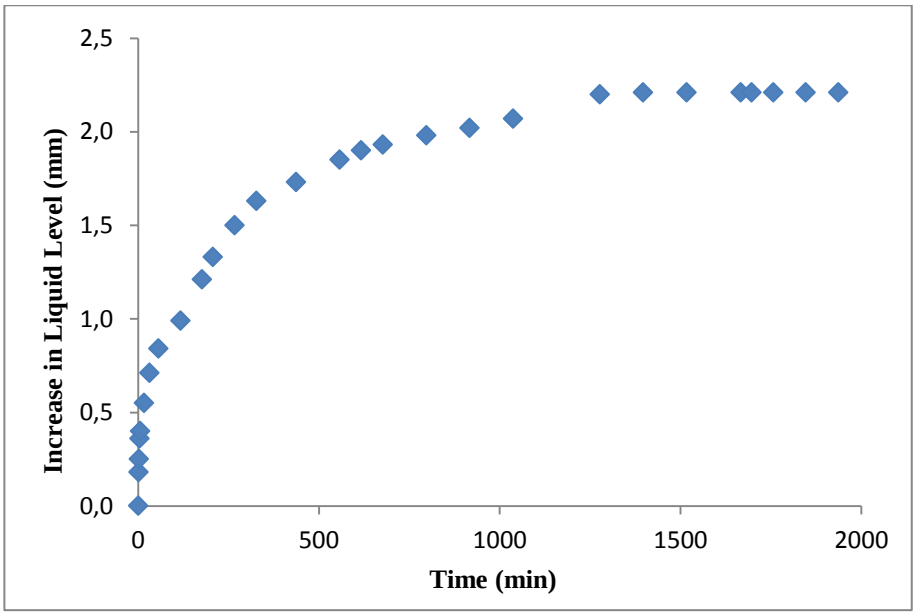


Figure 4.2. Change in the Position of the Liquid-Vapor Interface with Time (40 $^{o}$C and 739 psia (50.9 bar))

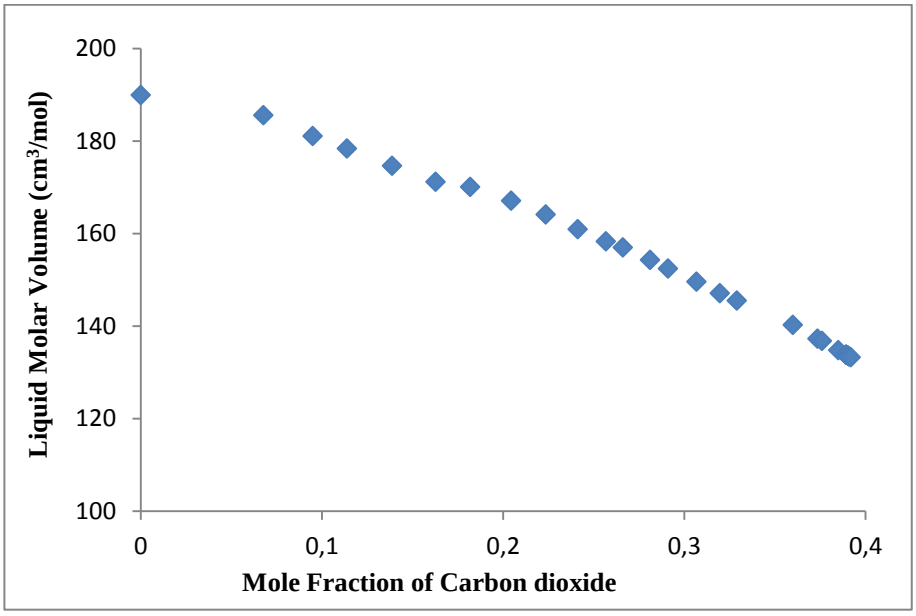


Figure 4.3. Change in the Liquid Molar Volume with Mole Fraction of Carbon dioxide in the Liquid Phase (40 $^{o}$C and 739 psia (50.9 bar))

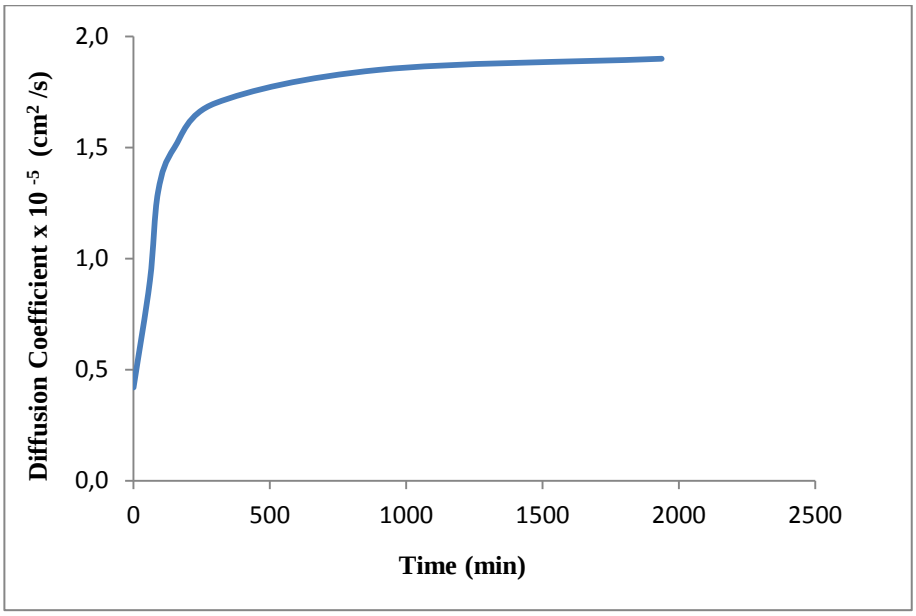


Figure 4.4. Liquid Phase Diffusion Coefficients (40 $^{o}$C and 739 psia (50.9 bar))

In Figure 4.1, the goodness of the fit is determined by calculating the $R^2$ value which is 0.9995. As shown in Figure 4.2, the liquid has expanded 2.21 mm in this run, and taking

this increase into account in calculations has caused 8.6% difference on the equilibrium mole fraction.

### 4.2. [bmim][$BF_4$] – $CO_2$ SYSTEM AT 313.15 K AND 1168 PSIA (80.5 BAR)

The data for the experimental run is given below. Liquid level and the mole fraction of $CO_2$ in liquid increase and reach equilibrium again as expected (see Figures 4.5 and 4.6). Mole fraction at equilibrium is found to be 0.516. The change in the liquid molar volume during the dissolution of carbon dioxide and the diffusion coefficients obtained by fitting the model to the experimental data are shown in Figures 4.7 and 4.8 respectively.

- Mass of the ionic liquid in the system: 9.2792 g
- Volume of carbon dioxide loaded to the system: 150.00 ml
- Initial volume of carbon dioxide in syringe pump: 264.80 ml
- Final volume of carbon dioxide in syringe pump: 109.70 ml
- Pressure of the system during the experiment: 1168 ± 2 psia
- Temperature of the system during the experiment: 40.0 ± 0.1 $^0$C

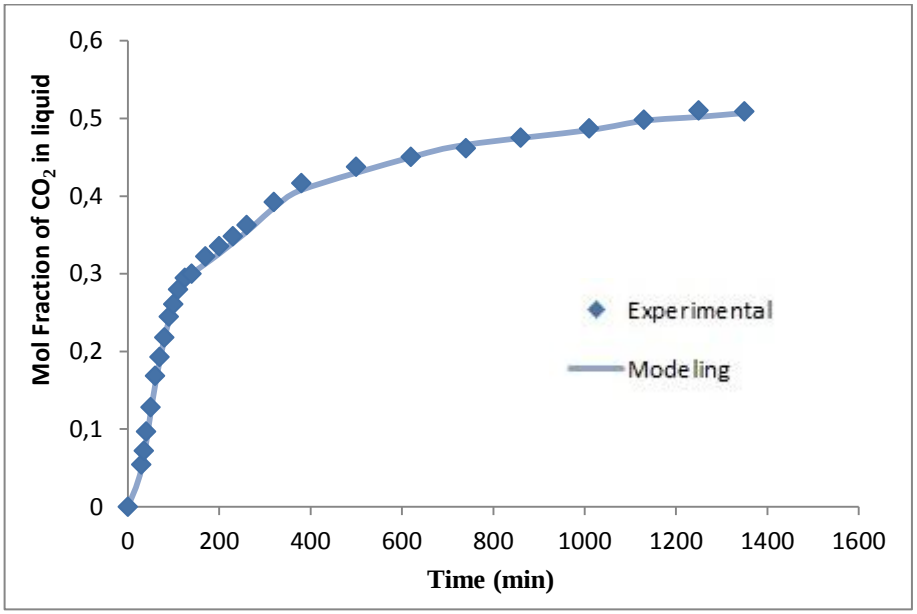


Figure 4.5. Average Carbon dioxide Mole Fractions in the Liquid Phase (40 $^o$C and 1168 psia (80.5 bar))

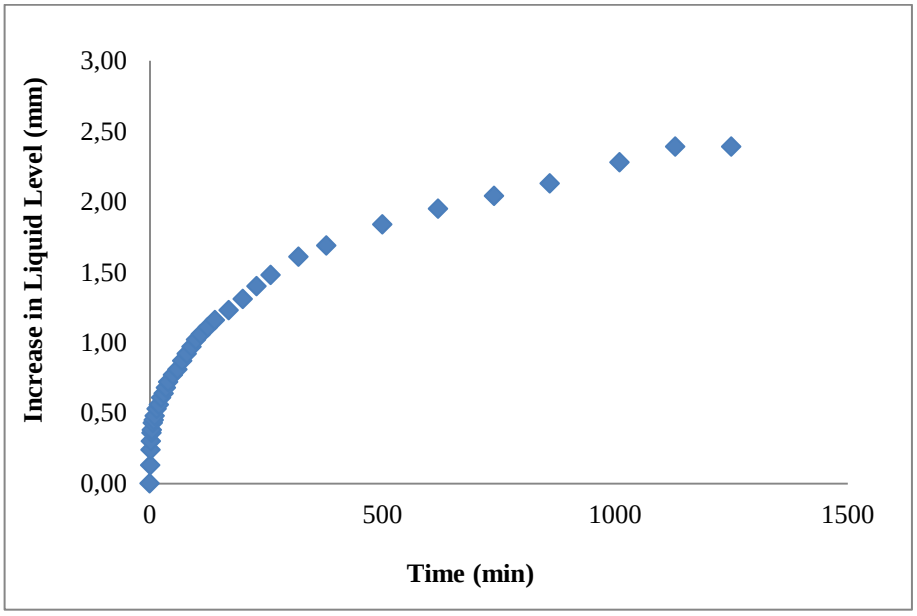


Figure 4.6. Change in the Position of the Liquid-Vapor Interface with Time (40 $^{o}$C and 1168 psia (80.5 bar))

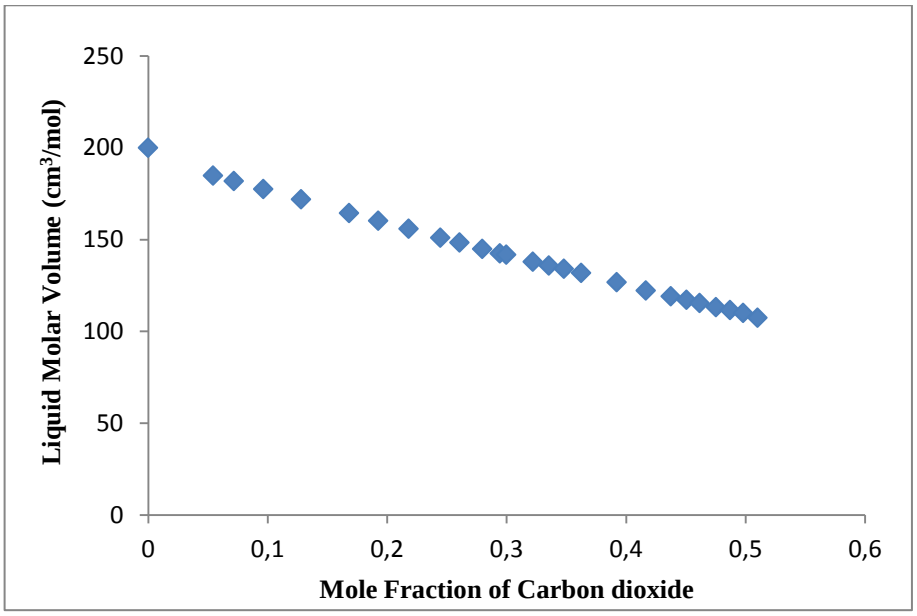


Figure 4.7. Change in the Liquid Molar Volume with Mole Fraction of Carbon dioxide in the Liquid Phase (40 $^{o}$C and 1168 psia (80.5 bar))

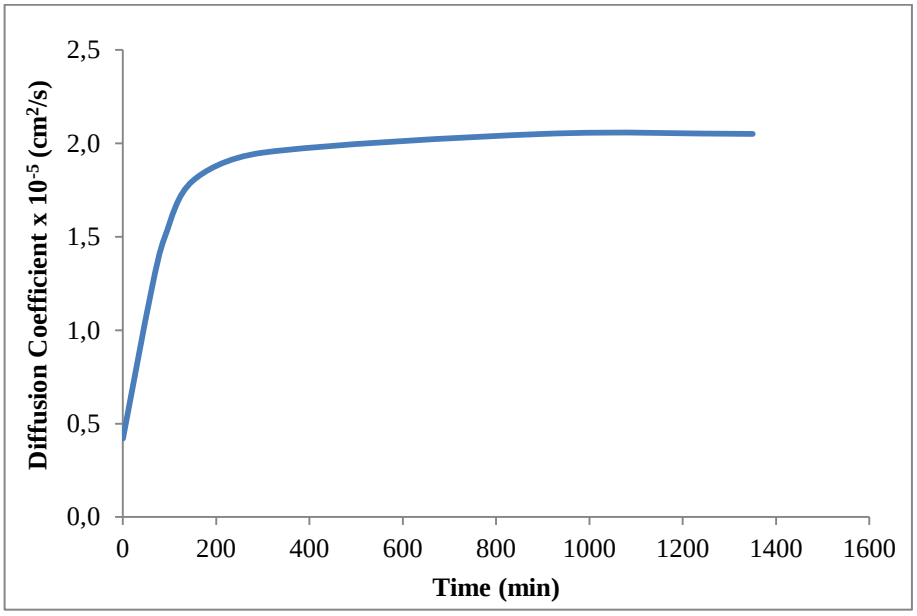


Figure 4.8. Liquid Phase Diffusion Coefficient (40 $^{o}$C and 1168 psia (80.5 bar))

In Figure 4.5, the goodness of the fit is determined by calculating the $R^2$ value which is 0.9991. As shown in Figure 4.6, the liquid has expanded 2.39 mm this time, and has caused 12.35% difference on the equilibrium mole fraction

### 4.3. [bmim][$BF_4$] – $CO_2$ SYSTEM AT 313.15 K AND 1483 PSIA (102.2 BAR)

The data for the experimental run is presented below. Liquid level and the mole fraction of $CO_2$ in liquid increase and reach equilibrium as expected (see Figures 4.9 and 4.10). Mole fraction at equilibrium is found to be 0.539. The change in the liquid molar volume during the dissolution of carbon dioxide and the diffusion coefficients obtained by fitting the model to the experimental data are shown in Figures 4.11 and 4.12 respectively.

- Mass of the ionic liquid in the system: 19.1286 g
- Volume of carbon dioxide loaded to the system: 136.96 ml
- Initial volume of carbon dioxide in syringe pump: 264.18 ml
- Final volume of carbon dioxide in syringe pump: 123.60 ml
- Pressure of the system during the experiment: 1483 ± 2 psia
- Temperature of the system during the experiment: 40.0 ± 0.1 $^{0}$C

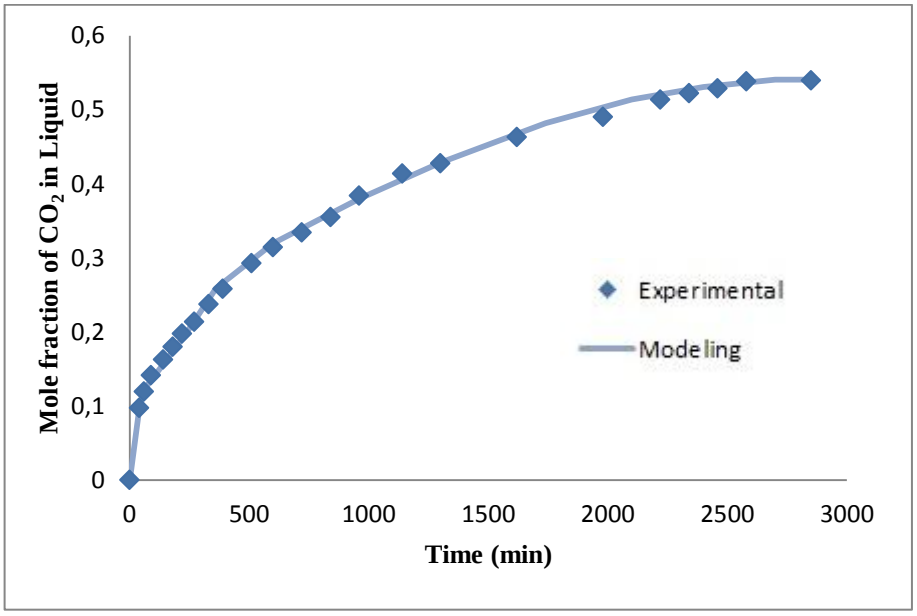


Figure 4.9. Average Carbon dioxide Mole Fractions in the Liquid Phase (40 $^{o}$C and 1483 psia (102.2 bar))

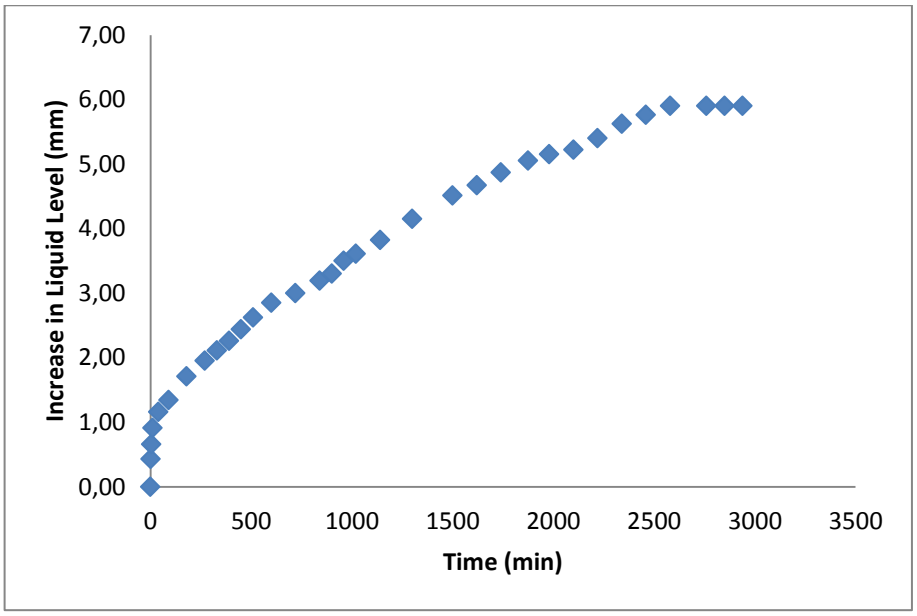


Figure 4.10. Change in the Position of the Liquid-Vapor Interface with Time (40 $^{o}$C and 1483 psia (102.2 bar))

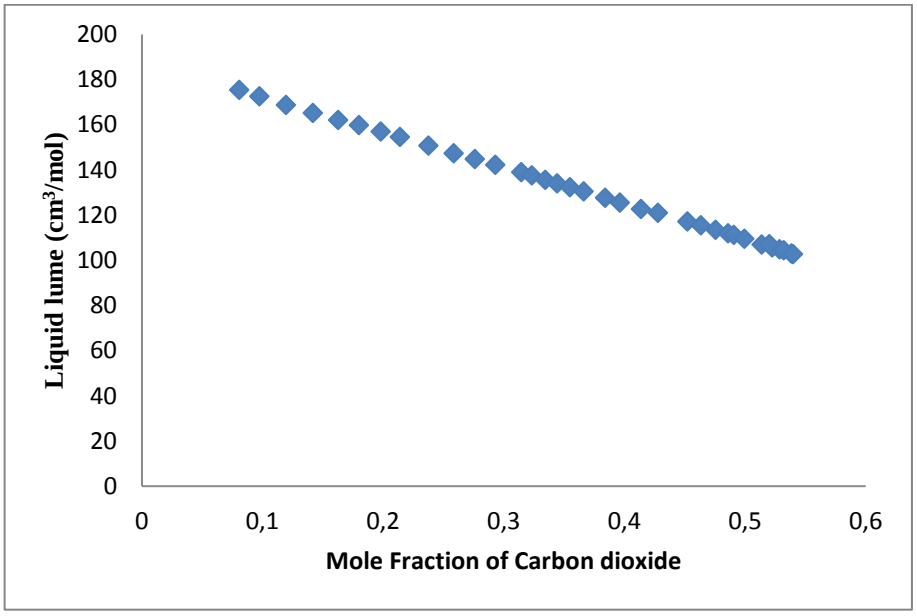


Figure 4.11. Change in the Liquid Molar Volume with Mole Fraction of Carbon dioxide in the Liquid Phase (40 $^{o}$C and 1483 psia (102.2 bar))

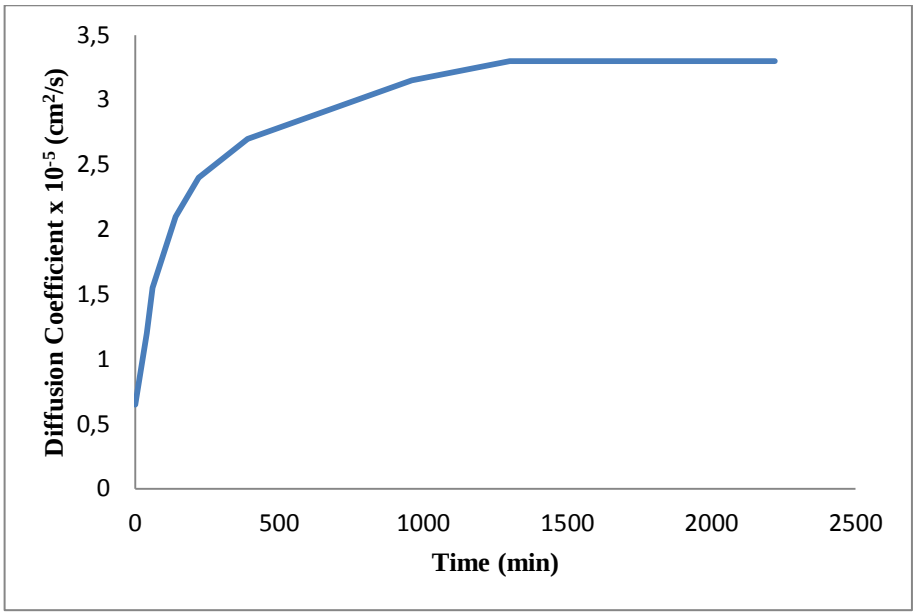


Figure 4.12. Liquid Phase Diffusion Coefficient (40 $^{o}$C and 1483 psia (102.2 bar))

In Figure 4.9, the goodness of the fit is determined by calculating the $R^2$ value which is 0.9993. As shown in Figure 4.10, the liquid has expanded 5.9 mm in this run, and has caused 30.69% difference on the equilibrium mole fraction.

### 4.4. [bmim][$BF_4$] – $CO_2$ SYSTEM AT 323.15 K AND 739 PSIA (50.9 BAR)

The data for the experimental run is given below. Liquid level and the mole fraction of $CO_2$ in liquid increase and reach equilibrium as expected (see Figures 4.13 and 4.14). Mole fraction at equilibrium is found to be 0.355. The change in the liquid molar volume during the dissolution of carbon dioxide and the diffusion coefficients obtained by fitting the model to the experimental data are shown in Figures 4.15 and 4.16 respectively.

- Mass of the ionic liquid in the system: 7.6262 g
- Volume of carbon dioxide loaded to the system: 135.67 ml
- Initial volume of carbon dioxide in syringe pump: 236.28 ml
- Final volume of carbon dioxide in syringe pump: 94.34 ml
- Pressure of the system during the experiment: 739± 2 psia
- Temperature of the system during the experiment: 50.0 ± 0.1 $^0$C

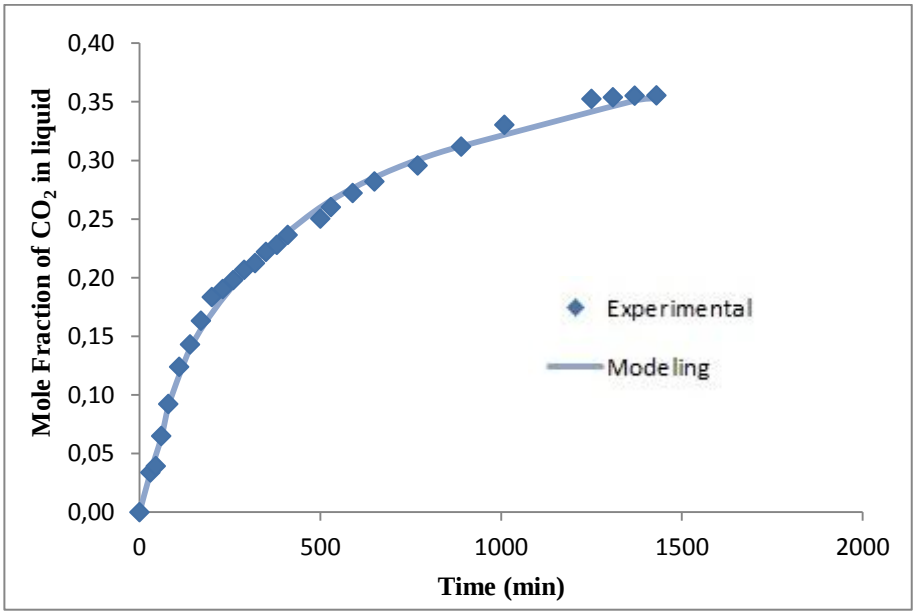


Figure 4.13. Average Carbon dioxide Mole Fractions in the Liquid Phase (50 $^o$C and 739 psia (50.9 bar))

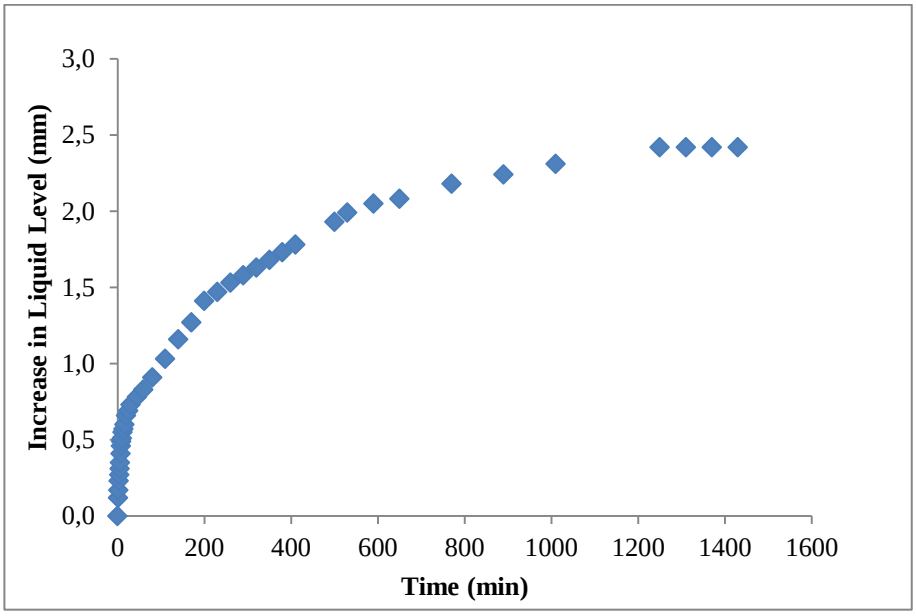


Figure 4.14. Change in the Position of the Liquid-Vapor Interface with Time (50 $^{o}$C and 739 psia (50.9 bar))

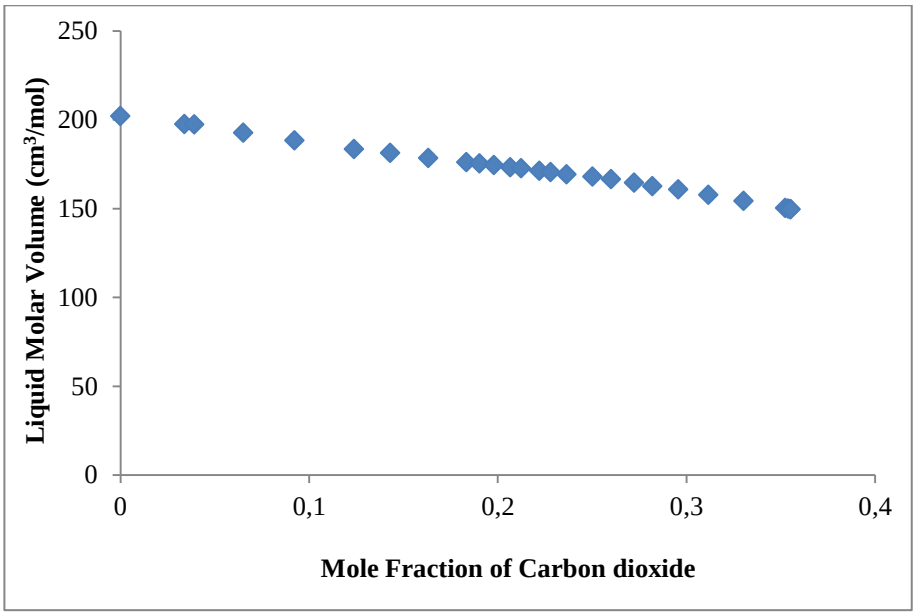


Figure 4.15. Change in the Liquid Molar Volume with Mole Fraction of Carbon dioxide in the Liquid Phase (50 $^{o}$C and 739 psia (50.9 bar))

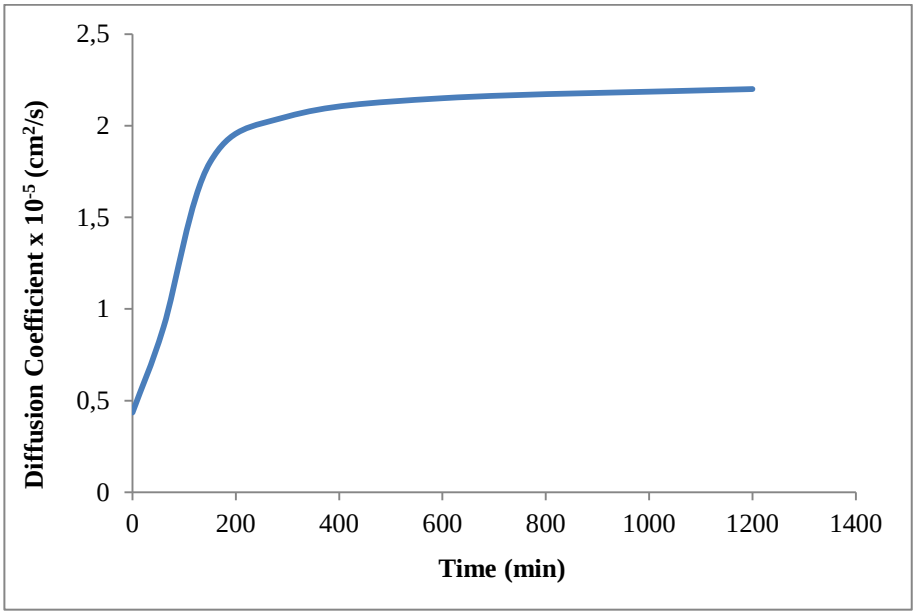


Figure 4.16. Liquid Phase Diffusion Coefficient (50 $^{o}$C and 739 psia (50.9 bar))

In Figure 4.13, the goodness of the fit is determined by calculating the $R^2$ value which is 0.9990. As shown in Figure 4.14, the liquid has expanded 2.42 mm in this run, and taking this into account in calculations 12.06% difference on the equilibrium mole fraction

## 4.5. [bmim][$BF_4$] – $CO_2$ SYSTEM AT 323.15 K AND 1149 PSIA (79.2 BAR)

The data for the experimental run is given below. Liquid level and the mole fraction of $CO_2$ in liquid increase and reach equilibrium as expected (see Figures 4.17 and 4.18). Mole fraction at equilibrium is found to be 0.443. The change in the liquid molar volume during the dissolution of carbon dioxide and the diffusion coefficients obtained by fitting model to the experimental data are shown in Figures 4.19 and 4.20 respectively.

- Mass of the ionic liquid in the system: 9.2443 g
- Volume of carbon dioxide loaded to the system: 154.34 ml
- Initial volume of carbon dioxide in syringe pump: 238.57 ml
- Final volume of carbon dioxide in syringe pump: 78.99 ml
- Pressure of the system during the experiment: 1149 ± 2 psia
- Temperature of the system during the experiment: 50.0 ± 0.1 $^{0}$C

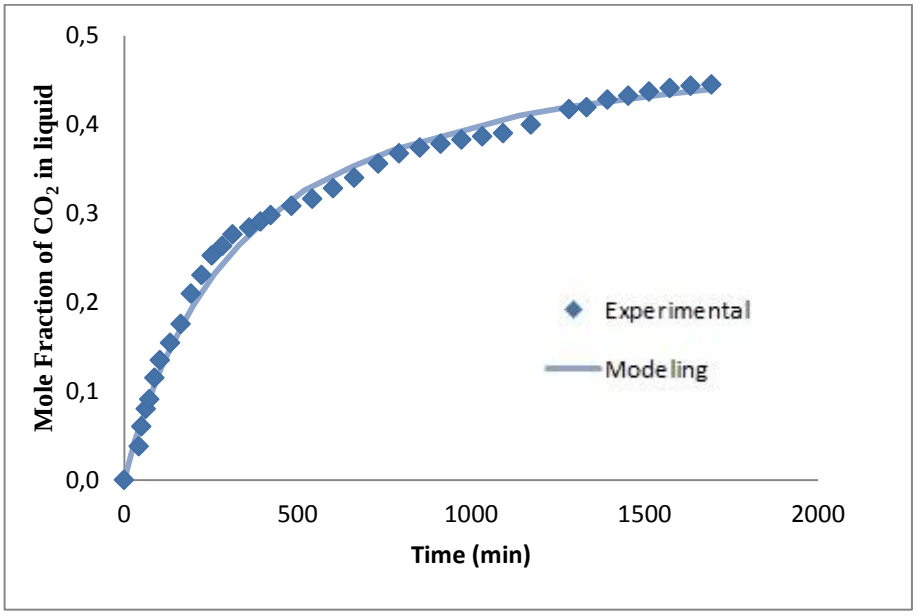


Figure 4.17. Average Carbon dioxide Mole Fractions in the Liquid Phase (50 $^{o}$C and 1149 psia (79.2 bar))

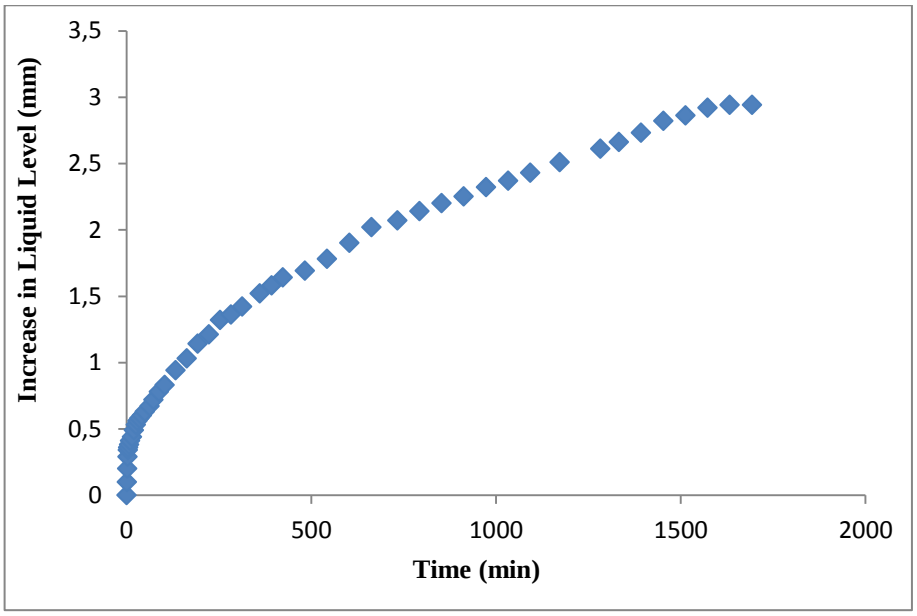


Figure 4.18. Change in the Position of the Liquid-Vapor Interface with Time (50 $^{o}$C and 1149 psia (79.2 bar))

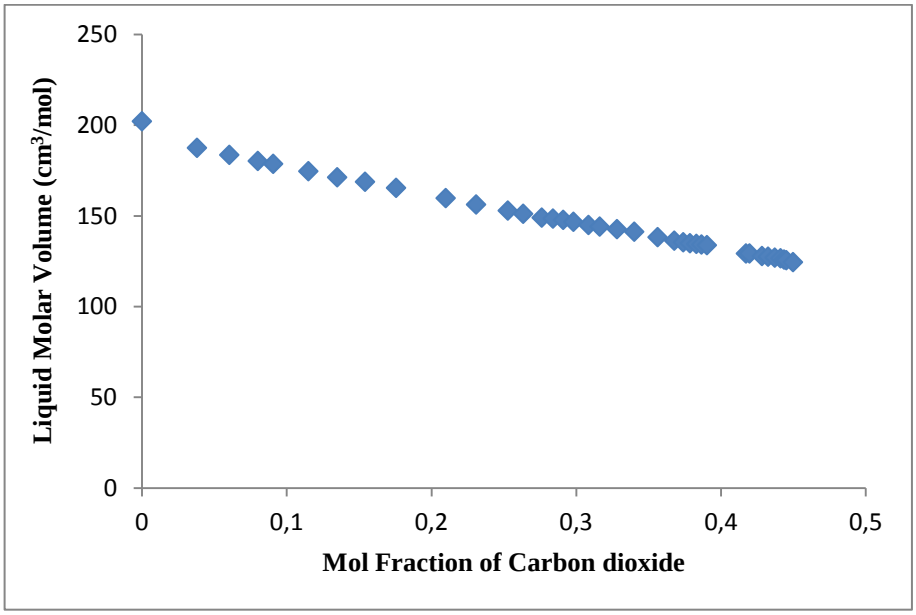


Figure 4.19. Change in the Liquid Molar Volume with Mole Fraction of Carbon dioxide in the Liquid Phase (50 $^{o}$C and 1149 psia (79.2 bar))

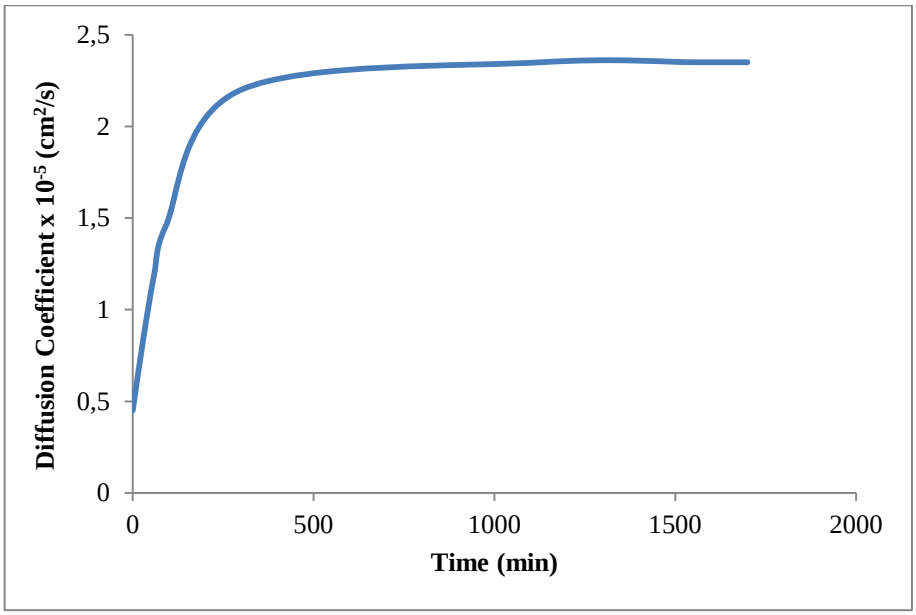


Figure 4.20. Liquid Phase Diffusion Coefficient (50 $^{o}$C and 1149 psia (79.2 bar))

In Figure 4.17, the goodness of the fit is determined by calculating the $R^2$ value which is 0.9911. As shown in Figure 4.18, the liquid has expanded 2.94 mm in this run, and has caused 15.88% difference on the equilibrium mole fraction.

### 4.6. [bmim][$BF_4$] – $CO_2$ SYSTEM AT 323.15K AND 1452 PSIA (100.1 BAR)

The data for the experimental run is given below. Liquid level and the mole fraction of $CO_2$ in liquid increase and reach equilibrium as expected (see Figures 4.21 and 4.22). Mole fraction at equilibrium is found to be 0.512. The change in the liquid molar volume during the dissolution of carbon dioxide and the diffusion coefficients obtained by fitting the model to the experimental data are shown in the Figures 4.23 and 4.24 respectively.

- Mass of the ionic liquid in the system: 14.231 g
- Volume of carbon dioxide loaded to the system: 140.87 ml
- Initial volume of carbon dioxide in syringe pump: 243.51 ml
- Final volume of carbon dioxide in syringe pump: 97.4 ml
- Pressure of the system during the experiment: 1452 ± 2 psia
- Temperature of the system during the experiment: 50.0 ± 0.1 $^0$C

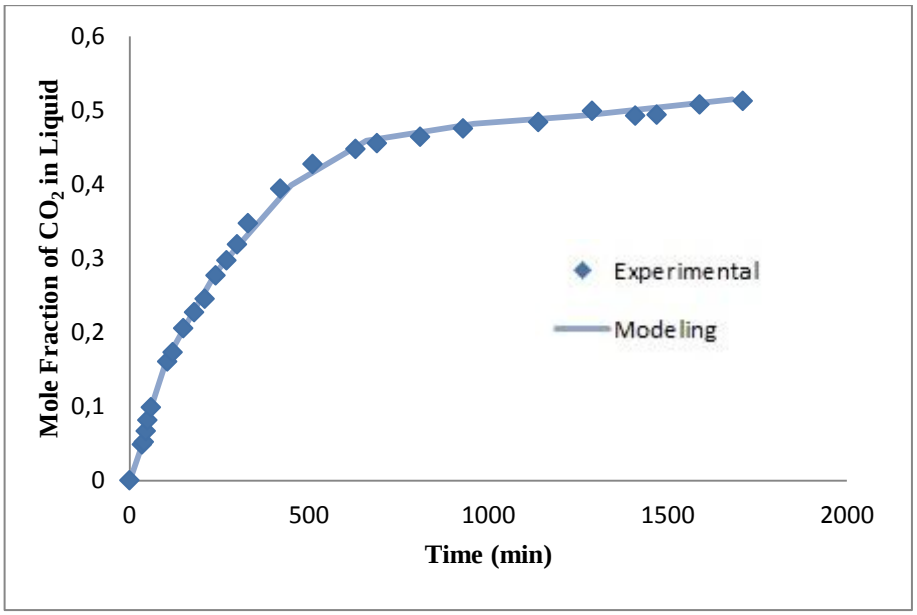


Figure 4.21. Average Carbon dioxide Mole Fractions in the Liquid Phase (50 $^o$C and 1452 psia (100.1 bar))

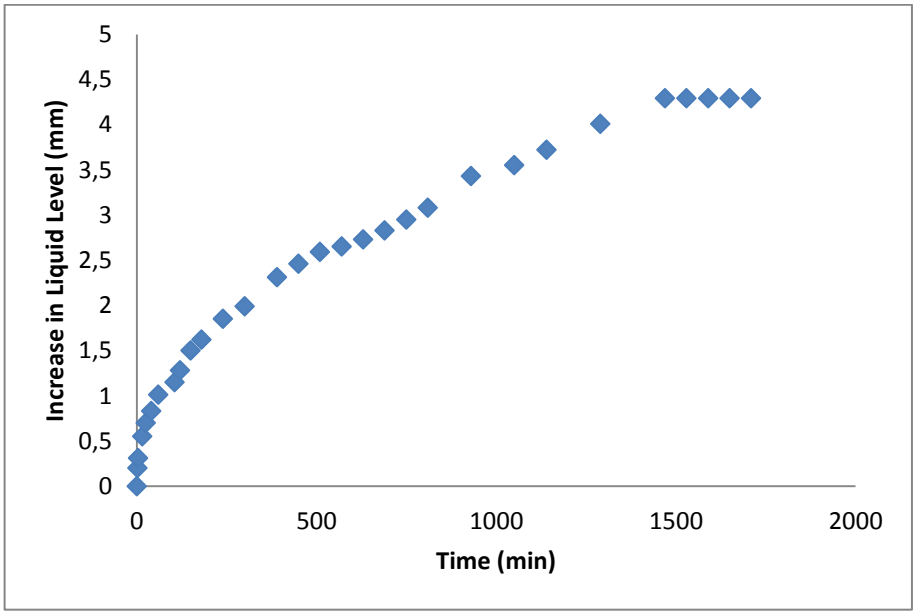


Figure 4.22. Change in the Position of the Liquid-Vapor Interface with Time (50 $^{o}$C and 1452 psia (100.1 bar))

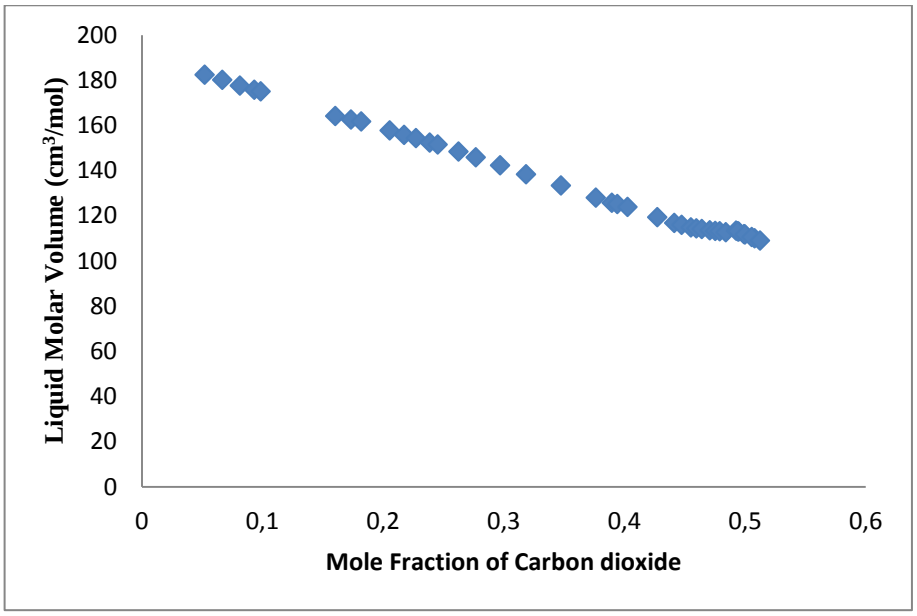


Figure 4.23. Change in the Liquid Molar Volume with Mole Fraction of Carbon dioxide in the Liquid Phase (50 $^{o}$C and 1452 psia (100.1 bar))

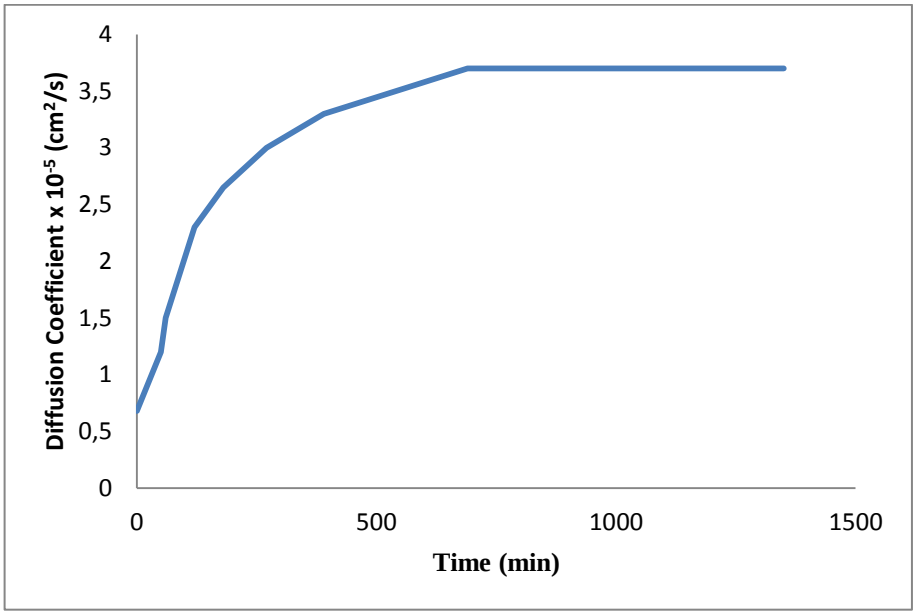


Figure 4.24. Liquid Phase Diffusion Coefficient (50 $^{o}$C and 1452 psia (100.1 bar))

In Figure 4.21, the goodness of the fit is determined by calculating the $R^2$ value which is 0.9993. As shown in Figure 4.22, the liquid has expanded 4.29 mm in this run, and has caused 19.62% difference on the equilibrium mole fraction

## 4.7. DISCUSSION

The validity of the results obtained in this study is evaluated using three approaches.

First, the thermodynamic equilibrium results are compared with literature. As shown in the following tables (Table 4.1 and 4.2), the results are similar to those reported by Aki et al. However, the solubility values determined by Lim et al. are quite higher.

Table 4.1. Comparison of the Thermodynamic Equilibrium Data ([bmim][$BF_4$], 313.15K)

| | 50 bar | 80 bar | 100 bar |
|---|---|---|---|
| Aki et al. | 0.40 | 0.51 | 0.54 |
| Lim et al. | 0.46 | 0.65 | 0.71 |
| Current work | 0.39 | 0.52 | 0.54 |

Table 4.2. Comparison of the Thermodynamic Equilibrium Data ([bmim][$BF_4$], 323.15K)

| | 50 bar | 80 bar | 100 bar |
|---|---|---|---|
| Aki et al. | 0.35 | 0.46 | 0.50 |
| Lim et al. | 0.38 | 0.57 | 0.62 |
| Current work | 0.35 | 0.45 | 0.50 |

Second, the initial values of high pressure diffusion coefficients are compared with the infinite dilution diffusivities reported in literature. For [bmim][$BF_4$]-$CO_2$ system at 313.15 K, Shiflett and Yokozeki found the infinite dilution diffusivity as 0.12 x $10^{-5}$ $cm^2/s$ while Hou and Baltus reported a value around 0.40 x $10^{-5}$ $cm^2/s$ which is closer to those obtained in this study ( see Figures 4.4, 4.8, and 4.12).

Table 4.3. Initial Values of Diffusion Coefficients ($10^{-5}$ $cm^2/s$)

| | 50 bar | 80 bar | 100 bar |
|---|---|---|---|
| 313.15 K | 0.42 | 0.42 | 0.65 |

As carbon dioxide dissolves in the ionic liquid, the viscosity of the liquid decreases. Equation 4.1 relates diffusivities to viscosities in a linear fashion and can be used for a rough estimation. Tomida et al.[41] measured that the viscosity of [bmim][$BF_4$]-$CO_2$ system at 313.15 K, 100 bar, decreased from 55.2 mPa to 12.9 mPa as the carbon dioxide mole fraction in the liquid increases from 0 to 0.43 (note that the equilibrium mole fraction at this temperature and pressure is 0.54). Therefore, based on these results, we think that it is reasonable to obtain equilibrium diffusivities much larger than the initial diffusivities.

$$D = \frac{D_0}{\eta/\eta_0} \tag{4.1}$$

# 5. CONCLUSIONS

In this study, experiments are carried out for [bmim][$BF_4$]-$CO_2$ system at different pressures (50-100 bar) and temperatures (313.15 K and 323.15 K). Using the experimental data and a computational fluid dynamics model, the changes in the diffusion coefficients during the process of carbon dioxide dissolution are determined at the aforementioned temperatures and pressures. The thermodynamic equilibrium mole fractions and the starting values of the calculated diffusion coefficients are found to be comparable to those reported in literature. The increase in the diffusion coefficients during the dissolution process is attributed to the decreases in the liquid viscosities.

The following directions are recommended for future work.

- Since the solubility of carbon dioxide in the ionic liquid decreases with the initial amount of water in the sample, the change in the diffusivities with water content is worth investigating.
- The ionic liquids which do not go through a significant viscosity change during the dissolution of carbon dioxide could also be examined. For example, diffusion coefficients in [bmim][$Tf_2N$]-$CO_2$ system could be studied in this context.
- The diffusion coefficient of carbon dioxide in ionic liquid mixtures (multi-component diffusion) is another direction for future work

# REFERENCES


1. Yang, Z., Pan, W., "Ionic liquids: Green solvents for nonaqueous biocatalysis", *Enzyme and Microbial Technology*, 2005;37, 19–28

2. Keskin, S., Talay, D., Akman, U., Hortaçsu, Ö., "A Review of Ionic Liquids towards Supercritical Fluid Applications", *Journal of Supercritical Fluids*, vol. 43, pp 150-180, 2007.

3. Ren, W., Sensenich, B., Scurto, A. M., "High-pressure Phase Equilibria of { Carbon Dioxide ($CO_2$) + n-alkyl-imidazolium bis(trifluoromethylsulfonyl)amide} Ionic Liquids", *J. Chem. Thermodynamics*, vol 42, pp 305-311, 2010

4. Welton, T., "Room temperature ionic liquids: Solvents for synthesis and catalysis", *Chem. Rev*. vol. 99, pp. 2071–2084, 1999.

5. Sugden, S., Wilkins, H., "The parachor and chemical constitution. Part. Fused metals and salts", *J. Chem. Soc*., 1291–1298, 1929

6. Gorman, J. "Faster, better, cleaner? New liquids take aim at old-fashioned chemistry", *Sci. News*, vol. 60, pp. 156–158, 2001.

7. Renner, R., "Ionic liquids: an industrial cleanup solution", *Environ. Sci. Technol*., vol. 35, pp. 410A–413A, 2001

8. Chiappe, C., Pieraccini, D. Review commentary; ionic liquids: solvent properties and organic reactivity, *J. Phys. Org. Chem*., vol. 18, pp. 275–297, 2005 .

9. Dupont, J,. "On the solid, liquid and solution structural organization of imidazolium ionic liquids", *J. Braz. Chem. Soc*., vol. 15, pp. 341– 350, 2004

10. Dai, S., DePaoli, D., Dietz, M., Mays, J., McFarlane, J., Steele, W., "Technical summaries on ionic liquids in chemical processing", *Chemical Industry Vision 2020 Technology Partnership Workshop*, 2003

11. Huddleston, J.G., Willauer, H.D., Swatloski, R.P., Visser, A.E., Rogers, R.D., "Room temperature ionic liquids as novel media for clean liquid–liquid extraction", *Chem. Commun*. (1998) 1765–1766.

12. Morland, R. "American Chemical Society Division of Industrial and Engineering Chemistry", in: Proceedings of the 221st American Chemical Society National Meeting, San Diego, 2001.

13. Zhao, H., Xia, S., Ma, P., "Review: use of ionic liquids as green solvents for extractions", *J. Chem. Technol. Biotechnol*., vol. 80, pp. 1089–1096, 2005.

14. Hutchenson, K. W., Scurto, A. M., Subramaniam, B., "Gas expanded Liquids and Near- Critical Media", *American Chemical Society*, USA, 2009

15. Arunajestesan, V., Wilson, K.A., Subramaniam, B., "Pressure-tuning the effective diffusivity of near-critical reaction mixtures in mesoporous catalyst", *Ind. Eng., Chem. Res*., vol. 42, pp. 2639-2643, 2003.

16. Subramaniam, B., Chaudhari, R., Chaudhari, A., Akien, G., Xie, Z., "Supercritical Fluids and gas-expanded liquids as tunable media for multiphase catalytic reactions", *Chemical Engineering Science,* USA, 2014

17. Shim- Pol A.M., Supercritical Fluid Technologies Inc, URL: http://shim-pol.pl/1,16,361-0-0-Supercritical_Fluid_Technologies_Inc.html

18. Siougkrou, E., Galindo, A., Adjiman, C. S., "On the Optimal Design of Gas-Expanded Liquids Based on Process Performance", *Chemical Engineering Science*, 2014.,

19. Jesop, P.G., Stanley, R.R., Brown, R.A., Eckert, C.A., Liotta, C.L., Ngo, T.T., "Neoteric solvents for asymmetric hydrogenation: supercritical fluids, ionic liquids, and expanded ionic liquids", *Green Chemistry*, vol. 5, pp 123, 2003

20. Krigmont, H. V. and Lumley, T. L., "Computational Fluid Dynamics Modeling", *Allied Environment Technologies* Inc., USA, 2007

21. Wendt, J. F., "Computational Fluid Dynamics – An Introduction" , 3rd ed., *Splinger*, Belgium, 2009

22. Tu, J., Yeoh, G. H., Liu C., Computational Fluid Dynamics- A Practical Approach, 1st ed., *Butterworth-Heinemann*, UK, 2008

23. Hirt, C.W. and Nichols, B.D., Volume of Fluid Method for the Dynamics of Free Boundaries, *Journal of Computational Physic*s vol. 39, 1981

24. Fluent Manual, UK, 2006

25. Biscarini, C., Di Francesco S., and Manciola P., "CFD Modeling Approach For Dam Break Studies", *Hydrology and Earth System Science,* Italy, 2009

26. Lim, B.H., Choe, W.H., Shim, J.J., Ra, C. S., Tuma, D., Lee, H., Lee, C. H., "High Pressure Solubility of Carbon Dioxide in Imidazolium-based Ionic Liquids with Anions [PF6] and [BF4]", *Korean J. Chem. Eng*., vol. 26, pp. 1130-1136, 2009

27. Moganty, S. S., Baltus, R. E., "Diffusivity of Carbon Dioxide in Room-Temperature Ionic Liquids", *Ind. Eng. Chem. Res*., vol. 49, pp. 9370-9376, 201).

28. Jalili, A. M., Mehdizadeha, A., Shokouhia, M., Ahmadia, A. N., Hosseini-Jenab, M., Fateminassaba, F., "Solubility and Diffusion of $H_2S$ and $CO_2$ in the ionic liquid 1-ethyl-3-methylimidazolium ethylsulfate", *J. of Chem. Thermodynamics*, vol. 42, pp. 1298-1303, 2010.

29. Hou, Y., Baltus, R. E., "Experimental Measurement of the Solubility and Diffusivity of CO2 in Room-Temperature Ionic Liquids Using a Transient Thin-Liquid-Film Method" , *Ind. Eng. Chem. Res*., vol. 46, pp. 8166-8175, 2007

30. Condemarin, R., Scovazzo, P., "Gas permeabilities, solubilities, diffusivities, and diffusivity correlations for ammonium-based room temperature ionic liquids with comparison to imidazolium and phosphonium RTIL data", *Chemical Engineering Journal*, vol. 147, pp. 51-57, 2011

31. Shiflett, M. B., Yokozeki A., "Solubilities and Diffusivities of Carbon Dioxide in Ionic Liquids: [bmim][$PF_6$] and [bmim][$BF_4$]", *Ind. Eng. Chem. Res*., vol. 44, pp. 4453-4464, 2005.

32. Xu, J., Wang, S., Yu, W., Xu, Q., Wang, W., Yin, J., "Molecular Dynamics Simulation for the Binary Mixtures of High Pressure Carbon Dioxide and Ionic Liquids", *Chinese Journal of Chemical Engineering*, vol. 22(2), pp. 153—163, 2014

33. Gong, Y., Wang, H., Chen, Y., Hu, Z., Li, Y., "A High-Pressure Quartz Spring Method for Measuring Solubility and Diffusivity of $CO_2$ in Ionic Liquids", *Ind. Eng. Chem. Res*., vol. 52, pp. 3926−3932, 2013

34. Banerjee, R., "Turbulent conjugate heat and mass transfer from the surface of a binary mixture of ethanol/iso-octane in a countercurrent stratified two-phase flow system", *International Journal of Heat and Mass Transfer*, vol. 51, pp. 5958-5974, 2008.

35. Banerjee, R., "A numerical study of combined heat and mass transfer in an inclined channel using the VOF multiphase model", *Numerical Heat Transfer Part A*, vol. 52, pp. 163-183, 2007.

36. Banerjee, R., Isaac, K. M., "An algorithm to determine the mass transfer rate from a pure liquid surface using the volume of fluid multiphase model", International *Journal of Engine Research*, vol. 5, pp. 23-37, 2004.

37. NIST Chemistry Webbook, URL: http://webbook.nist.gov/chemistry/

38. Hou, Y., Baltus, R. E., "Experimental Measurement of the Solubility and Diffusivity of $CO_2$ in Room-Temperature Ionic Liquids Using a Transient Thin-Liquid-Film Method", *Ind. Eng. Chem. Res*., vol. 46, pp. 8166-8175, 2007

39. Gonzalez-Miquel, M., Bedia, J., Abrusci, C., Palomar, J., Rodriguez, F., "Solubility and Diffusivity of CO2 in [hxmim][$NTf_2$], [omim][$NTf_2$], and [dcmim][$NTf_2$] at T = (298.15, 308.15, and 323.15) K and Pressures up to 20 bar", Jour*nal of Chemical and .Engineering Data*, vol. 59, pp. 212-217, 2014.

40. Morgan, D., Ferguson, L., Scovazzo, P., "Diffusivities of Gases in Room-Temperature Ionic Liquids: Data and Correlations Obtained Using a Lag-Time Technique", *Ind. Eng. Chem. Res*., vol. 44, pp. 4815-4823, 2005.

41. Tomida, D., Kumagai, A., QiaO, K., Yokoyama, C., "Viscosity of 1-butyl-3-methylimidazolium tetrafluoroborate + $CO_2$ mixture", *J. Chem. Eng*, vol. 37, pp.81-89, 2008.

# APPENDIX A: SAMPLE CALCULATION FOR EQUILIBRIUM MOLE FRACTION AT 323.15 K AND 739 PSIA (50.9 bar)

A sample calculation for equilibrium mole fraction is carried out for [bmim][$BF_4$]-$CO_2$ system at 50 $^oC$ and 739 psia as shown below;

- Mass of the ionic liquid in the system: 7.6262 g
- Volume of carbon dioxide loaded to the system: 135.67 ml
- Initial volume of carbon dioxide in syringe pump: 236.28 ml
- Final volume of carbon dioxide in syringe pump: 94.34 ml
- Pressure of the system during the experiment: 739 psia (50.9 bar)
- Temperature of the system during the experiment: 50,0 $^0C$
- Increase in the liquid level at equilibrium: 2.42 mm

The number of $CO_2$ in liquid is calculated by using equation A.1

$$n_{i,isco} = n_{CO_2} + n_{f,isco} + n_{f,jer} \quad (A.1)$$

Final volume of carbon dioxide in Jerguson cell is equal to theinitial volume of carbon dioxide in Jerguson view-cell minus the expanded liquid volume.

Final volume of carbon dioxide at gas phase in Jerguson: 135.67– (5.55*0.242)= 134.33 ml
Volume of carbon dioxide dissolved in the liquid: 236.28-94.34-134.33=7.61 ml
Number of moles of carbon dioxide in the liquid: 7.61/409.3= 0.01859 mole
Number of moles of the ionic liquid: 7.6262/226.02= 0.03374 mole

Here, 409.3 is the molar volume of carbon dioxide at given temperature and pressure. 226.02 is the molecular weight of the ionic liquid and the equilibrium mole fraction of carbon dioxide in the liquid is equal to 0.3553.

# APPENDIX B: ESTIMATION OF EXPERIMENTAL ERROR

The accuracy of the experimental result depend on the accuracy of each instrument. The sample calculation to estimate the total error is carried out for [bmim][$BF_4$]-$CO_2$ system at 50 $^oC$ and 739 psia (50.9 bar) as shown below;

At 323.15 K and 739 psia (50.9 bar), the equilibrium mole fraction of carbon dioxide in the liquid is equal to 0.3553

The error margin of ISCO pump is 0.01 ml [23]. the final volume of carbon dioxide in liquid is between 7.59 and 7.63 ml and mole fraction of carbon dioxide in liquid was calculated for this values is 0.3547 and 0.3559 respectively. So the error of ISCO pump volume reading is ±0.0006.

The accuracy of pressure transducer is ±2psi. the molar volume of carbon dioxide at 737 and 741 psia is 410.49 and 407.82 $cm^3$/mole respectively. The mole fraction of carbon dioxide was calculated as 0.3544 and 0.3561 and the error is ±0.0009.

The accuracy of thermocouple is ±0.1 ºC. the error was calculated as ±0.0002 by using molar volume at 50.1 and 49.9 ºC.

The accuracy of cathetometer is ±0.01 mm. 2.41 and 2.43 mm changed equilibrium mole fraction ±0.002.

The total error margin is ±0.002 and equilibrium mole fraction can be expressed as 0.355 ±0.002